T.C.
ISTANBUL UNIVERSITY
INSTITUTE OF HEALTH SCIENCES

MASTER THESIS

INVESTIGATION OF CD70-CD27 RELATED MOLECULAR MECHANISMS IN TUMOR MICROENVIRONMENT OF NON-SMALL CELL LUNG CANCER

MERVE SAİDE UZUNOĞLU

SUPERVISOR
PROF. DR. İLHAN YAYLIM

MEDICAL BIOTECHNOLOGY PROGRAMME
DEPARTMENT OF MOLECULAR MEDICINE

İSTANBUL-2019

THESIS APPROVAL

YÜKSEK LİSANS TEZİ ONAYI

İstanbul Üniversitesi Sağlık Bilimleri Enstitüsü, İ.Ü. Aziz Sancar Deneysel Tıp Araştırma Enstitüsü Moleküler Tıp Anabilim Dalı, Moleküler Tıp Yüksek Lisans Programı öğrencisi **Merve Saide UZUNOĞLU**'nun tarafından **Prof. Dr. İlhan YAYLIM** 'ın danışmanlığında hazırlanan **"Küçük Hücreli Dışı Akciğer Kanserli Hastalarda CD70/CD27 Molekülleri ile İlişkili Mekanizmaların İncelenmesi"** başlıklı tez aşağıdaki jüri üyeleri tarafından 30/09/2019 tarihinde yapılan Tez Savunma Sınavında başarılı bulunmuş ve Yüksek Lisans Tezi olarak kabul edilmiştir.

Jüri Başkanı
(Danışman)
Prof. Dr. İlhan YAYLIM
İ.Ü.Aziz Sancar DETAE
Moleküler Tıp Anabilim Dalı

Jüri

Prof. Dr. Akif TURNA
İ.Ü.Cerrahipaşa –CTF Göğüs
Cerrahisi A.D.

Jüri

Prof. Dr.Ali Osman GÜROL
İ.Ü. Aziz Sancar DETAE,İmmünoloji
Anabilim Dalı

Jüri

Prof. Dr. Arzu ERGEN
İ.Ü.Aziz Sancar DETAE
Moleküler Tıp Anabilim Dalı

Jüri

Dr. Öğr. Üyesi Yemliha YILDIZ
İstinye Üni. Tıp Fak.
Tıbbi Biyoloji A.D

DECLARATION

I declare that this study is an individual work in which there was no unethical behavior during all the stages from planning the thesis until its writing and that all the information in this thesis was obtained according to academic and ethical rules. I declare that I have referenced all the information and interpretations not obtained in this study and that these sources are listed in the list of sourced and that there is no violation of patent or copyrights during the study and the writing of the thesis.

Merve Saide Uzunoğlu

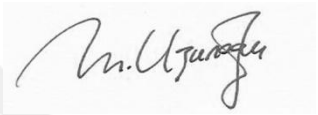

DEDICATION

I dedicate this thesis

To my Mother, Ayşe Uzunoğlu
To my Father, İbrahim Kemal Uzunoğlu

and

To my Brother, Melih Muhammed Uzunoğlu.

ACKNOWLEDGMENTS

Firstly, I want to thank my supervisor Prof. Dr. İlhan Yaylım for her guidance, time and efforts that she provided me during my master thesis project. Also, I thank my co-supervisor Assoc. Prof. Dr. Özlem Küçükhüseyin for her kindness, support, and good-humor. Also, my special thanks to research associate Mehmet Tolgahan Hakan and Ph.D. student Dilara Sönmez for their kindness and help during my project.

I declare sincere appreciation to Prof. Dr. Akif Turna for providing patient samples and follow-up data for this project.

My greatest and strongest and truly thanks goes to my twin sister Aylin Uzunoğlu who is the one and the only person I went through all the real difficulties and hard times together.

This Project was supported by Istanbul University Scientific Research Projects Committee. Project No: TYL-2018-29527

TABLE OF CONTENTS

LIST OF TABLES

LIST OF FIGURES

LIST OF ABBREVIATIONS

NSCLC: Non-small cell lung cancer

TME: Tumor microenvironment

TNFSF: Tumor necrosis factor super family

sCD27: Soluble CD27

WHO: World Health Organization

AIS: Adenocarcinoma in situ

MIC: Minimally invasive carcinoma

SCLC: Small cell lung carcinoma

SqCC: Squamous cell carcinoma

ECM: Extracellular matrix

CAFs: Cancer-associated fibroblasts

VEGF: Vascular endothelial growth factor

FGFs: Fibroblast growth factor

PDGF: Platelet-derived growth factor

TGF-β: Transforming growth factor-beta

SDF1: Stromal cell-derived factor 1

HIFs: Hypoxia-inducible factors

DCs: Dendritic cells

NK cells: Natural killer cells

TILs: T infiltrating lymphocytes

CTLs: Cytotoxic T cells

Tregs: Regulatory T lymphocytes

MDSC: Myeloid-derived suppressor cell population

CTLA-4: Cytotoxic T-lymphocyte antigen-4

PD-1: Programmed cell death protein 1

PD-L1: Programmed cell death protein ligand 1

RCC: Renal cell carcinoma

SDS-PAGE: Sodium dodecyl sulfate-polyacrylamide gel electrophoresis

ÖZET

Uzunoğlu MS. Küçük Hücreli Dışı Akciğer Kanserli Hastalarda CD70/CD27 Molekülleri ile İlişkili Mekanizmaların İncelenmesi. İstanbul Üniversitesi Sağlık Bilimleri Enstitüsü, Moleküler Tıp ABD. Yüksek Lisans. İstanbul. 2019

CD70, TNF süper ailesinin üyesi olan ve reseptörü CD27 antijenine bağlanarak önemli immünolojik roller üstlenen, olgun dendritik hücreler ile T ve B lenfositlerinde eksprese edilen, kanser gelişimi ve ilerlemesinde yer alan bir tip II transmembran eş-uyarıcı molekülüdür. Normal dokularda CD70 ekspresyonu görülmezken, çeşitli tümör tiplerinde CD70 aşırı ekspresyonu tespit edilmiştir. Hematolojik maligneler ve çeşitli solid kanser türlerinde aşırı ekspresyonu görülmüşse de küçük hücreli dışı akciğer kanseri (KHDAK) ile yapılmış çalışmalar kısıtlıdır. KHDAK dünya çapında en ölümcül kanser türü olarak konumunu korumaktadır. Bununla birlikte akciğer kanseri tanısı temel olarak histopatolojik analizlere dayanıyor olsa da, yeni tanı ve prognostik biyobelirteçlerin araştırılması her geçen gün devam etmektedir. Bu çalışma, CD70, CD27, FOXP3 ve CD3 moleküllerinin KHDAK dokularındaki ekspresyon durumu ile birlikte hastaların serumda çözünebilir CD27 (sCD27) seviyelerinin, kanser teşhisi için bir tanısal biyobelirteç olarak potansiyel kullanımını değerlendirildi. Tümör mikroçevrede protein ekspresyon durumları, Western Blot ile 32 KHDAK dokusu için analiz edildi ve ELISA ile KHDAK hastalarının serumunda sCD27 seviyeleri incelendi. CD70'in, dokuların %15,63'nde ekspres oluğu bulundu. CD27 ekspresyonu %75, FOXP3 %43,75, CD3 %87,5 olarak tespit edildi. sCD27 seviyesi KHDAK'lı hastalarda anlamlı ölçüde yüksek bulundu ($p < 0,0001$). sCD27'nin hastalığın tespiti için tanısal bir potansiyel biyobelirteç olarak kullanılabileceği sonucuna ulaşıldı. CD27, FOXP3 ve CD3 için toplam hasta numunelerindeki yüksek pozitiflik yüzdesi, CD70 ekspresyonu ile ilişkilendirilmedi. Ayrıca, başka bir anlamlı sonuç ise yüksek sCD27 seviyesi ile CD70 ekspresyonu gösteren örnekler arasında bulundu ($p = 0,007$). Bu sonucun, tümör mikroçevredeki CD70-CD27 etkileşimi sonucunda CD27'nin kesilerek seruma gönderildiği bilgisini doğruladı görüldü.

Anahtar Kelimeler: Küçük hücreli dışı akciğer kanseri, CD70, CD27, tümör mikroçevre, Western Blot

Bu çalışma, İstanbul Üniversitesi Bilimsel Araştırma Projeleri Birimi tarafından desteklenmiştir. Proje No: TYL-2018-29527

ABSTRACT

Uzunoğlu MS. Investigation of CD70-CD27 Related Molecular Mechanisms In Tumor Microenvironment of Non-Small Cell Lung Cancer. İstanbul Üniversitesi Sağlık Bilimleri Enstitüsü, Moleküler Tıp ABD. Yüksek Lisans. İstanbul. 2019

CD70 is known as tumor necrosis factor superfamily (TNFSF) molecule and ligand of another TNFSF costimulatory molecule of CD27. Immune cells are the cells that CD70 is expressed transiently, whereas CD70 expression has not been found in normal tissue cells. Although several types of cancer showed CD70 positivity correlated with patient outcome, non-small cell lung cancer (NSCLC) requires further investigation. This study was designed to evaluate expression status of CD70, CD27, FOXP3 and CD3 in tumor microenvironment (TME) of NSCLC tissues, and the potential usage of soluble CD27 (sCD27) levels in serum as a diagnostic biomarker for cancer diagnosis. Protein expressions in TME were analyzed for 32 NSCLC tissues by Western Blot. sCD27 levels in serum of NSCLC patients were detected with ELISA. CD70 expression was found in 15.63% of overall samples. CD27 expression was detected in 75%, FOXP3 in 43.75%, CD3 in 87.5% in samples. sCD27 serum level was found significantly higher ($p<0.0001$) for the patient group with very high sensitivity (90%) suggesting that sCD27 has a potential usage as a diagnostic biomarker for NSCLC for detection of the disease. Only a few NSCLC cases showed CD70 expression in TME. A high percentage of positivity in overall patient samples for CD27, FOXP3, and CD3 was not correlated with CD70 expression. Also, high level of sCD27 gave a significant result for CD70 positivity ($p=0.007$) suggesting CD70-CD27 interaction may cause CD27 cleavage and release to serum in CD70+ tumors in NSCLC.

Keywords: Non-small cell lung cancer, CD70, CD27, tumor microenvironment, Western Blot

This Project was supported by Istanbul University Scientific Research Projects Committee. Project No: TYL-2018-29527

1. INTRODUCTION AND AIM

Lung cancer is a very severe type of tumor and has a high rate of occurrence and death for both sexes worldwide. NSCLC forms the bigger part of the cases among the other types of lung tumors. Disease symptoms become visible when cancer already gets an advance level. Thus, developing precise biomarkers that permit detection and diagnosis for correct evaluation of the patient characteristics is crucial. CD70 has been shown that it is a very promising target as a potential marker for NSCLC. [1]–[4]

CD70 has a costimulatory signaling pathway in the tumor microenvironment through a receptor-ligand interaction. CD70 is expressed on several immune cells. Tightly regulated expression of CD70 is desirable in terms of T cell and B cell activation. However, different tumor types have been shown abnormal CD70 expression resulting in immune system evasion in TME. Although, CD27, one of the TNFSF molecule, shows no expression on normal or tumor cells, CD27 expression is restricted with only immune cells. CD70/CD27 pathway has an impact on the function and recruitment of different types of T cells in TME which has a substantial place in immune escape mechanism in TME. Also, when CD27 receptor interacts with its ligand, CD27 has split apart from T cells and soluble CD27 (sCD27) releases into the serum which is found that an increased level of sCD27 is detected in patient sera and related with patient histopathological characteristics and patient outcome. [5]–[9]

The aim was to seek for relevancy of CD70/CD27 axis and immune recruitment in TME of NSCLC together with patient outcome and clinicopathological characteristics of patients. In addition, both tissue and adjacent normal tissue expressions and association of CD70, CD27, CD3 and FOXP3 molecules wanted to be revealed for NSCLC. Furthermore, the sCD27 level in NSCLC patients was investigated to reveal the possible usage of sCD27 to be used as a marker.

2. GENERAL INFORMATION

2.1. Lung Cancer And Its Epidemiology

Cancer ranks among the remarkably prevalent death factor worldwide and acceleration in the incidence and mortality of cancer each year make it a current issue of the world. Estimated new cases in 2018 for cancer were 18.1 million and the estimated number of deaths caused by cancer was near to the 9.6 million around the world with regard to the data of World Health Organization (WHO) data. [1], [2], [10]

Lung cancer keeps its position at the top of the list among all cancers for incidence and mortality for both sexes (2 million cases) which contribute 12.3% of the total number of new cases and 1.8 million cancer-related deaths, contributing 18.4% of cancer deaths worldwide in 2018. According to the latest cancer data of WHO, lung cancer was responsible for the highest number of cancer cases and the majority of deaths in men in the world. Among females, lung cancer came after breast and colorectal cancer for the rate of occurrence, contributing 8.4% of all cases. It leads to a high number of deaths the most right after breast cancer (13.8%) in 2018. [1], [2], [3]

Developed countries have the highest rates of occurrence and lung cancer-related deaths which are connected with some risk factors associated with socioeconomic development. The global burden will increase according to the estimation of WHO because of increasing tobacco use, carcinogenic exposure, and environmental toxins. Moreover, the highest rate of incidence for lung cancer is mostly seen at the age between 65 years-old and 84 years-old worldwide. Also, in the patient group younger than 40, lung cancer incidence remains very low. [1], [3], [4], [11]

2.2. Classification Of Lung Cancer

Lung cancer has been categorized by WHO into 2 main groups as small cell lung carcinoma (SCLC) and non-small cell lung carcinoma. Also, NSCLC where consists of 85% of all cases, has 3 subgroups. Adenocarcinoma is the common one. Squamous cell carcinoma (SqCC) and large cell carcinoma are the other subtypes. Also, there are several variants in these clinical subtypes. In addition, the new WHO classification distinguishes lung cancer into groups but the heterogenic structure of lung cancer has been found even in the same subtype. [3], [4], [11]–[13]

2.2.1. Adenocarcinoma

Adenocarcinoma consists of 40% of all lung cancer cases. Alveolar cells in the smaller airway epithelium are the main location where adenocarcinoma first starts. TTF-1 and napsin A are two main pathological biomarkers. In respect to the last WHO classification in 2015, adenocarcinoma is divided into 3 subtypes depending on the level of spreadability. While adenocarcinoma in situ (AIS) is a 30 mm or smaller carcinoma, minimally invasive carcinoma (MIA) has a diameter less than 30 mm with an invasion size of less than 5 mm. Tumor necrosis, lymphovascular invasion, or pleural invasion factors in the tumor may cause completely different diagnosis for MIA, even though all sizes fit with the definition for MIA diagnosis. [3], [4], [11], [13], [14]

2.2.2. Squamous cell carcinoma

Roughly 30% to 25 % of lung tumors are SqCC which firstly forms in airway epithelium in the lungs. Patients with SqCC mostly come with a history of smoking. Its pathological markers are p40, CK5, and CK6. [3], [4], [11], [13], [14]

2.2.3. Large Cell Carcinoma

It represents only a small portion of all lung cancers with 10% to 15%. It's characteristic of appearing, growing and spreading quickly in any part of the lung makes the treatment very difficult for patients. [3], [4], [11], [14]

2.3. Diagnosis Of NSCLC

Diagnosis of NCSLC at early stage delays for most of the patients because of the lack of symptoms which most of them start appearing when the disease already gets an advance level. As a matter of fact that symptoms are even misevaluated at the advanced stage of cancer because of the similarity with other diseases symptoms such as some infectious diseases. Diagnostic indications are mainly cough, dyspnea, coughing up blood, and chest pain. [3], [4], [11], [15], [16]

Imaging, laboratory, and biomarker tests, biopsies and medical histories have been using for diagnosis of NSCLC. Even though imaging tests tell a lot about lung cancer presence, it does not give a definite answer to whether a patient has lung cancer. Chest X-rays, CT (computed tomography) scan, MRI (magnetic resonance imaging) scan, PET (positron emission tomography) scan, and bone scan are one of the imaging tests to diagnose lung cancer. Furthermore, biopsy gives the most definite result. In

addition to biopsy, biomarker tests provide important information about the NSCLC situation. [4], [11], [12], [16], [17]

2.4. Stages Of NSCLC

After the diagnosis of NSCLC, the patient goes under a staging process which mainly tells about the situation of cancer in the lung to determine the best way of treatment. Mainly, the TNM system is used for staging NSCLC. T refers to tumor magnitude, and N is for expansion to lymph nodes. Metastasis is represented by M. [4], [16], [18]–[21]

Table 2-1. Stages of NSCLC. [4], [16], [18]–[21]

Stages	Features
Stage 0:	The stage where the tumor has started to develop but has not spread yet to other places which are also called in situ stages. TNM status is Tis, N0, M0.
Stage I:	The stage where the primary tumor has occurred but not spread to the lymph node and not have metastasis to other organs. According to the dimension, stage I has two substages as SIA and SIB. SIA tumors have a diameter of ≤3 and SIB tumors are between 3cm and 4 cm in size. TNM status is T1, N0, M0 for SIA and T2, N0, M0 for SIB.
Stage II:	This stage has also two substages as SIIA and SIIB regarding the dimension of the tumor. While SIIA represents a tumor with a dimension between 4 cm and 5 cm with no lymph node metastasis, a tumor at the SIIB stage has a dimension larger than 5 cm and smaller than 7 cm with lymph node metastasis. TNM status is T2, N0, M0 for SIIA and T1-2-3, N0-1, M0 for SIIB.
Stage III:	IT has 3 substages as SIIIA, SIIIB, and SIIIC. There is no distant organ metastasis at any substages of stage III but tumor spreads to different lymph nodes in the chest. TNM status is T1-2-3-4, N1-2, M0 for SIIIA, T1-2-3-4, N2-3, M0 for SIIIB, and T3-4, N2-3, M0 for SIIIC. Tumor size for stage III is between 5 cm and 7 cm. Also, surgery mostly is not applicable to tumors at this stage.

Stage IV:	The stage where the tumor has spread to other lung and/or any distant organs such as liver, brain, and bones via the bloodstream. Stage IV has two substages as SIVA and SIVB. TNM status is T1-2-3-4, N1-2-3, M1 for SIVA and T1-2-3-4, N1-2-3, M1 for SIVB.

2.5. Tumor Microenvironment

Tumor microenvironment (TME) is a heterogenic formation of cells and structures where mainly refers the surrounding habitat of tumor cells including blood vessels, fibroblast, immune cells, extracellular matrix (ECM), inflammatory cells, etc. (Figure 1). Tumor always stays in touch with the environment in order to maintain and grow itself in its location which creates different signals and effects that also help to suppress the immune system and promote angiogenesis. Continuous interaction between tumor cells and their microenvironment promotes tumor progression, invasion, and metastasis. Furthermore, TME has an important place to investigate treatment options in order to understand the level of progression and drug resistance capability of cancer, meaning that the clinical importance of TME is fundamental for the diagnosis and treatment of cancer. [22]–[26]

While stroma in normal conditions has a capacity to prevent tumorigenesis for the survival of the tissues and organs and acts as a defense mechanism, tumor cells use stroma in their favor to promote their growth in TME. Stroma cells are supportive cells around the tissue compose of fibroblasts and other supportive cells, in which the structure goes into an alteration after tumorigenesis. Altered stroma in TME starts generating growth factors, chemokines, and cytokines that promote cancer progression. This structural change of stroma, immune cell compositions and immune response in TME are tightly regulated by the tumor to keep the tumor cells drug-resistant. [23], [25]–[28]

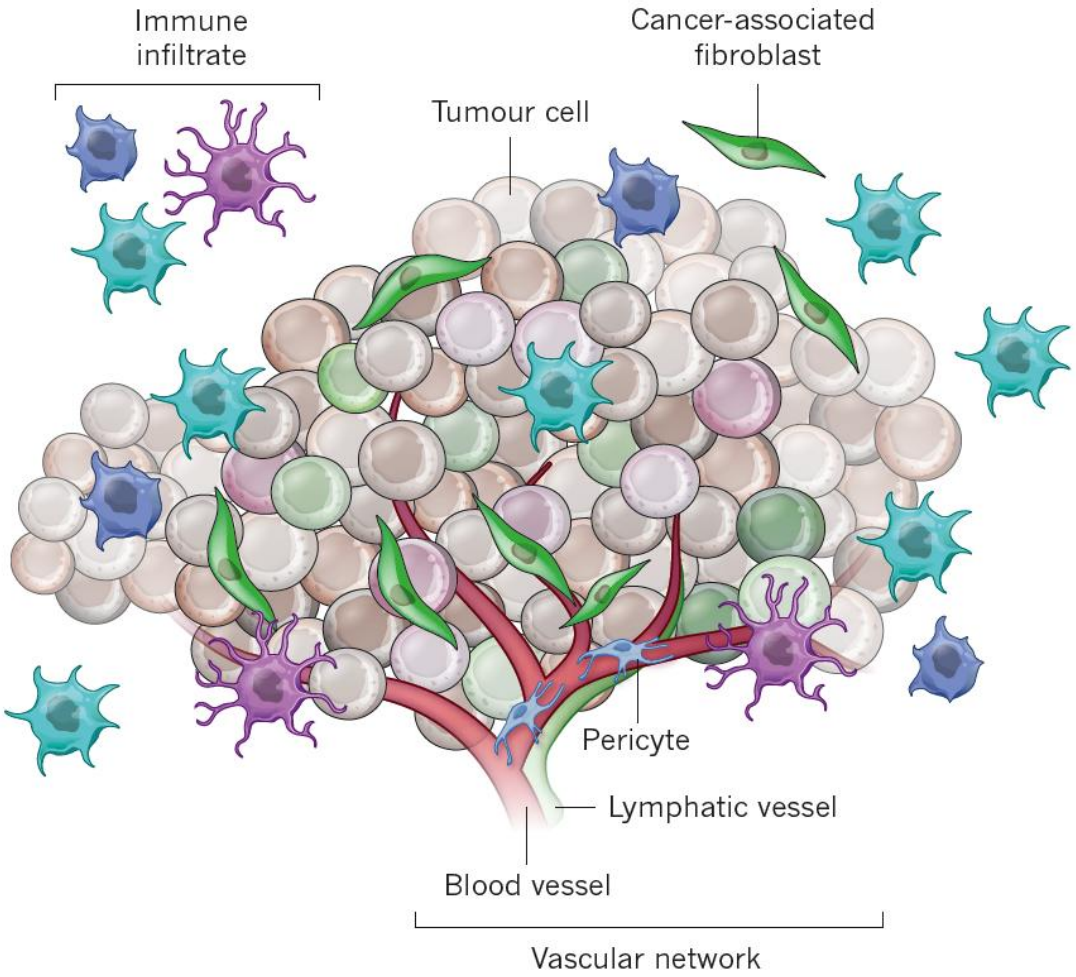

Figure 2-1. A representation of a heterogenic structure of tumor microenvironment with tumor cells and their surroundings by immune cells, cancer-associated fibroblasts, and blood vessels. [25]

2.5.1. Cancer-associated fibroblasts (CAFs)

Fibroblasts are connective tissue cells that are responsible for the production of ECM and collagen and suppress tumor formation in which they undergo a structural change by tumor and become cancer-associated fibroblasts that stimulate cancer viability. CAFs have a heterogenic structure in TME, that secrete vascular endothelial growth factor (VEGF), fibroblast growth factor (FGFs), platelet-derived growth factor (PDGF), transforming growth factor-beta (TGF-β), stromal cell-derived factor 1 (SDF1) and other angiogenic signals. Furthermore, CAFs promote cancer metastasis and suppress immune cells in TME. All these characteristics of CAFs make them a really good target for cancer therapy. [22], [25], [28]–[30]

2.5.2. Vascular Networks in TME

Angiogenesis is a very well-controlled mechanism that refers to a complex vessel formation from preexisting vessels with endothelial cells along the inside. On the other hand, vasculogenesis refers to a new vessel formation by the recruitment of circulating endothelial progenitor cells. Regulating of the mechanism and structure of angiogenesis is important for both viability of cancer and potential cancer therapy, in which it is controlled by several molecules, signals, and their receptors as well, such as VEGFs and VEGFRs, FGFs and FGFRs, PDGF-β and PDGFR-β, etc.. One of the most crucial regulators is hypoxia-inducible factors (HIFs) which acts as a transcription factor and activate angiogenesis in TMA. [25]–[27], [29]–[33]

The vascular network provides a heterogenic structure in TME where tumors promote themselves and escape the immune system with several distinct mechanisms. Thus, vascular density is fundamental to predict prognosis for poor outcome in several tumors such as NSCLC and colorectal cancer. [25], [27], [29]–[32]

2.5.3. Immune Cell

It is a well-known fact that the immune system protects the body from any possible damage or infections by the help of both innate and adaptive immune system. Tumor formation is one of the threats that should be avoided by the immune system in the body. However, tumors have the ability to suppress the immune system and survive. In the normal condition of tumorigenesis, a group of immune cells is recruited into the TME, but heterogeneity differs among tumor types, locations or stages of the tumor. Both CAFs and vascular networks play crucial roles in the mechanism or level of suppression or activation of immune cells in the TME together with tumor cells. [25], [26], [38], [27]–[30], [34]–[37]

Immune cells that infiltrate to TME has two main characteristic defense mechanism which is known as innate and adaptive immune response. Natural killer cells (NK), dendritic cells (DC), macrophages are innate immune cells and it conducts itself as a primer of defense for the threats. Adaptive immune cells are T infiltrating lymphocytes (TILs; cytotoxic T cells (CTL) and T helper cells) and B cells which come as the second line of defense. While CTLs can directly kill the tumor, regulatory T lymphocytes (Tregs) can suppress CTLs. Tumor cells inhibit the cytotoxic effect of T cells and promote immunosuppression by expressing ligands of T-cell receptors which

have an activator function on T-cells once they interact with their ligands. These types of molecules are called immune checkpoint molecules and they are fundamental in TME. Blocking strategies have been developing for immune checkpoint molecules for cancer therapy. Tumors also result in immune suppression by recruiting myeloid-derived suppressor cell population (MDSC) into the TME to make the environment immunosuppressive for T-cells. Moreover, MDSC promotes growth factor secretion by CAFs resulting in angiogenesis and recruitment of T regulatory cells (Tregs) into the TME, resulting inhibition of NK cells function and expansion of effector T-cells. Tumor-associated macrophages also locate in TME and affect tumor progression. [25], [27], [29], [30], [34]–[39]

2.6. Tumor Microenvironment In NSCLC

It has been shown that TME is an important place for NSCLC to seek immunity-related mechanisms to evaluate the prognostic status of cancer. Several specialized immune cells, for instance, cytotoxic T cells and helper T cells rank among the factors that have predictive value for the diagnosis of NSCLC. Also, different molecules that involve in immune system-related signal pathways result in immune suppression by specific interactions with immune cells in TMA. Thus, these types of molecules and signal pathways have been investigating for cancer therapy as potential biomarkers and targeted pathways. Recent studies have shown that there are 13 different types of immune cells in NSCLC and T cells are the dominant immune cell types in the TME. T cells take a fundamental part in the tumor progress that has been revealed that T cells in NSCLC predict progression, stages and treatment options of cancer. [5], [38]–[43]

2.6.1. Immune Checkpoints in NSCLC

The understanding of tumors is vital in order to overcome cancer but it is even more important to understand better the microenvironment and immune cells in the TME. Tumor finds ways to escape the immune system and costimulatory and coinhibitory pathways related to immune checkpoints are the once that cancer uses in its favor. Moreover, a major attack is performed by cytotoxic T cells against tumor cells in TME after they are activated by specific pathways. Once specific antigens get recognized by immune cells, the antitumor effect is generated in the TME. However, the tumor uses these costimulatory or coinhibitory signals that directly affect T cell function in the end. In NSCLC, several immune checkpoints have been characterized

until now. Cytotoxic T-lymphocyte antigen-4 (CTLA-4), programmed cell death protein 1 (PD-1) and programmed cell death protein ligand 1 (PD-L1) are the major immune checkpoint inhibitory molecules in NSCLC. Also, immune checkpoints inhibitors (ICIs) have been developed for cancer immunotherapy in order to blockade the immune checkpoint molecules and prevent tumors to escape immune system by using these pathways In addition to these, checkpoints can be investigated for NSCLC such as CD70/CD27 pathway of costimulation in TME. [39], [43]–[49]

2.6.2. CD70 related mechanisms in NSCLC

CD70, tumor necrosis factor superfamily (TNFSF) molecule, is a ligand of TNFSF costimulatory molecule, CD27. They are both employed costimulation of immune cells and their expression is tightly controlled to generate correct signaling Activated T cells and B cells, and DCs are the immune cells in which CD70 is expressed transiently, whereas CD70 expression has not been found in normal tissue cells. Different cancer types have been screening for CD70 expression and some solid tumor and hematologic malignancies have been found positive for CD70. Renal cell carcinoma (RCC) is a strong positive for expression of CD70 among solid tumors followed by glioblastoma. [7]–[9], [50]–[53]

Receptor molecule CD27 is expressed on T cells, B cells and NK cell, which is responsible for the proliferation of T cells, differentiation of memory T cells, and proper activation of T cells, and also differentiation of plasma cells, maturation of B cells and production of immunoglobulins with CD70/CD27 signaling pathway. [6]–[9], [50]–[54]

3. MATERIAL AND METHOD

3.1. Data and Sample Collection

Surgically removed primary tissue samples from 32 NSCLC patients were obtained as well as serum samples from 30 NSCLC patients and 32 healthy controls were collected together with the clinicopathological data and demographic data from Istanbul Training and Research Hospital. In order to use patients samples and data in the study, ethical approval was obtained from the ethical committee of Istanbul University Hospital.

3.2. Tissue Sample Preparation and Protein Isolation

3.2.1. Preparation and Homogenization of Tissue Samples with TRIzol

TRIzol® Reagent (TRIzol® Reagent, Ambion by Life Technologies, Cat. no. 15596-026) was used for protein isolation from tissue samples. The homogenization of samples was performed following the reagent protocol. TRIzol® Reagent was stored at room temperature (RT) for longer usage. Homogenization was performed at RT with 50-100 mg of frozen tissue samples taken from -80º C and thawed on ice and 1 ml of TRIzol® Reagent in a fume hood. All homogenized samples were stored at -80º C before phase separation.

3.2.2. Phase Separation and Protein Isolation

Stored samples were allowed to thaw for 5 min at RT for phase separation. 200 µl of chloroform was added into a tube and the tube was capped carefully. Then, the tube was shaken by hand for 15 seconds. Samples were incubated at RT for 2-3 minutes and then tubes were centrifugated at 12,000 x g for 15 minutes at 4º C. After phase separation occurred into a red phenol-chloroform phase, interphase and an upper aqueous phase were collected for protein isolation. Any aqueous phase overlying onto the interphase was completely removed. 300 µl of 100% ethanol was added onto the samples and the tubes were inverted several times to allow mixing. After incubation of samples at RT for 2-3 minutes, the tubes were centrifugated at 2000 x g for 5 minutes at 4º C. Then, phenol-ethanol supernatant was collected into a new tube for protein isolation.

1.5 mL of isopropanol was added to the phenol-ethanol supernatant and samples were incubated at RT for 10 minutes. In order to precipitate the protein, samples were centrifugated at 12,000 x g for 10 minutes at 4º C and the supernatant was discarded.

3.2.3. Protein Wash and Protein Resuspension

0.3 M guanidine hydrochloride in 95% ethanol was used as a washing solution to wash protein pellet. 2 mL of wash solution was added to the pellet and samples were incubated at RT for 20 minutes. Then, centrifugation was performed at 7500 x g for 5 minutes at 4º C and the supernatant was discarded. Protein washing was repeated for two more times.

After the third wash was completed, 2 mL of 100% ethanol was added to the protein pellet and mixed by vortex. 20-minute incubation of samples at RT followed by centrifugation of tubes at 7500 x g for 5 minutes at 4ºC and supernatant was discarded. Then, protein pellet was allowed for air drying for 5-10 minutes.

200 µl of 1% SDS was added to the protein pellet by pipetting up and down until the pellet was resuspended completely. Protein resuspension was centrifugated at 12,000 x g for 10 minutes at 4ºC to sediment any insoluble material in the resuspension. After that, the supernatant containing protein was transferred to a new tube and stored at 20ºC for further usage.

3.3. Determination of Concentration with BCA Kit

Determination of protein concentration of isolated tissue samples was performed with the SMART BCA Protein Assay Kit (Cat. No. 21071). Before the assay, all samples were diluted together with standards and then 25 µl of each standard and samples were added to the wells of flat bottom 96-well plate. The plate was incubated at 37 degrees for half an hour after adding 200 µl of working solution which was prepared in 50:1 dilution and covered with aluminum foil. OD values were measured at 562 nm. The concentration of all samples was calculated according to the plotted curve.

3.4. SDS-PAGE and Western Blot

3.4.1. SDS-PAGE

3.4.1.1. Preparing Protein Samples for SDS-PAGE

Isolated protein samples were used for sodium dodecyl sulfate-polyacrylamide gel electrophoresis (SDS-PAGE) and Western Blot experiments to detect CD70, CD27, CD3, FOXP3 expressions on tissues. In order to load an equal amount of protein into each well of SDS-PAGE gel, protein concentration was determined and 200 µg of protein samples were prepared for each sample to load each well.

Optiblot LDS Sample Buffer (4X, Abcam, ab119196) was used to prepare samples for SDS-PAGE running. Samples were denaturated at 95º C for 10 minutes before loading the samples into the wells.

3.4.1.2. Running SDS-PAGE

10% separating gel and 5% stacking gel were prepared in house for each SDS-PAGE running as indicating in Table 3-1.

Table 3.1. 10% Separating gel and 5% Stacking gel formulation.

10% Separating Gel	**10 ml**	**5 ml**
Distilled water	4 ml	2 ml
%30 Acrylamide	3.3 ml	1.65 ml
1.5 M Tris-HCl (pH 8.8)	2.5 ml	1.25 ml
%10 SDS	0.1 ml	50 µl
%10 APS	0.1 ml	50 µl
TEMED	4 µl	2 µl
5% Stacking Gel	**5 ml**	**2 ml**
Distilled water	3.4 ml	1360 µl
%30 Acrylamide	0.83 ml	332 µl
1 M Tris-HCl (pH 6.8)	0.63 ml	252 µl
%10 SDS	0.05 ml	20 µl
%10 APS	0.05 ml	20 µl
TEMED	5 µl	2 µl

Mini-Protean® Tetra System (Bio-Rad) and Mini Trans-Blot® Cell System (Bio-Rad) were used for running of SDS-PAGE and protein blotting respectively. The vertical electrophoresis set was obtained, all glasses and combs were cleaned with 70% ethanol and dried before gels were prepared. Then, the vertical electrophoresis set was assembled. 10-well combs were used for each SDS-PAGE running.

After gels were placed into the tank, tank was filled with running buffer up to the specified level. 10X TGS Running Buffer (Bio-Rad, Cat. no. 161-0732) was used to prepare 1X running buffer to run SDS-PAGE.

20 µl of prepared protein samples and 3.5 µl of protein standard (Bio-Rad, Precision Plus Protein™ Dual Color Standards, #1610374, 10–250 kD) were loaded to the wells. SDS-PAGE run was performed at 50 V for 15 minutes. Then, the voltage was increased to 150 V and the run was finished in 1 hour.

After running was completed, gels were removed from their cassette. Stacking gel and wells were removed and only separating gel part was transferred to a box filled with distilled water for blotting.

3.4.2. Western Blot

3.4.2.1. Wet Transfer

10X TG Transfer Buffer (Bio-Rad, Cat. no. 161-0734) was used to prepare 1X transfer buffer. Also, 1X transfer buffer was prepared in house as well following the formula (Table 3-2) and stored at 4º C.

Table 3-2. Formulation of 1X transfer buffer.

Transfer Buffer	1X
Tris	3.03 g
Glycine	14.4 g
Methanol 100%	200 ml
ddH_2O	800 ml

Gels were placed in 1X transfer buffer for 5-10 min. filter papers and sponges were wetted with 1X transfer buffer before assembling the stack. Immun-Blot® PVDF

Membrane Sandwiches (Bio-Rad, Cat. no. 162-0219) were prepared before transfer. PVDF membrane was activated in 100% methanol for 2 minutes and transferred into 1X transfer buffer for equilibration for 5 minutes. The transfer sandwich was assembled by placing the membrane on the cathode and the gel on anode between sponges and filter papers. Any possible bubbles in the stack were removed with a roller before the cassette was closed. The cassette and an ice block were placed into the tank. Then, the tank filled with precooled 1X transfer buffer.

The transfer was done in a cold room (4º C) at 100V, 350 mA for 1 hour. When the transfer was completed, the cassette holder was removed from the tank and the transfer stack was disassembled carefully. Gels were placed in Bio-Safe™ Coomassie Blue Stain (Bio-Rad, Cat. no. 1610786, g-250) for dying the left protein in the gel to check transfer efficiency. The membrane was proceeded for blocking step.

3.4.2.2. Blocking the Membrane and Antibody Incubation

5% skimmed milk in Tris-buffered saline with Tween 20 (TBST) buffer was prepared as a blocking solution. After blotting, the membrane was washed ones with TBST and incubated with blocking solution at RT for 1 hour on a shaker.

Primary antibody incubation was performed overnight at 4°C on a shaker with the appropriate dilutions in blocking solution (5% skimmed milk in TBST) by following manufactures instruction with Rabbit polyclonal Anti-CD70 Antibody (Abcam, ab175389, 1:2000), Rabbit polyclonal Anti-beta-actin Antibody (Abcam, ab119716, 1:5000), Rabbit polyclonal Anti-CD27 Antibody (Abcam, ab70103, 1µg/1ml) Rabbit polyclonal Anti-FOXP3 Antibody (Abcam, ab70103, 1:500), and Rabbit polyclonal Anti-CD3 Antibody (Abcam, ab70103, 0.5 µg/1ml).

After overnight primary antibody incubation, the membrane was washed four times with TBST for 5 minutes each. The membrane was incubated with secondary antibody solution using Goat polyclonal Secondary Antibody to Rabbit IgG - Fc (HRP) (Abcam, ab97069) prepared in blocking solution (5% skimmed milk in TBST) with an appropriate antibody dilution (1:5000) by following manufactures instruction at RT for 1 hour.

Secondary antibody incubation was followed by washing three times for 5 minutes and once for 15 minutes with TBST at RT. Clarity™ Western ECL Substrate

Kit (Bio-Rad, Cat. no. 1705060) was used as a substrate for chemiluminescent detection. The substrate was prepared according to the manufacturer's instructions and applied to the membrane. Chemiluminescent signals were captured using CCD camera-based imager.

3.5. ELISA for Determination of CD27 Level in Patients Serum

Human sCD27 INSTANT ELISATM Kit (ThermoFisher Scientific) was provided for enzyme-linked immunosorbent assay (ELISA) for quantitative detection of human soluble CD27 (sCD27) level in 30 serum samples collected from 30 NCSLC patients and 32 serum samples collected from healthy controls. ELISA was carried out according to the manufacturer's instructions.

Serum samples were stored frozen at -20º C and they brought to the RT right before the experiment. ELISA plate was used directly after removal from –20º C. Serum samples were prediluted 1:25 with Sample Diluent provided in the kit by following this dilution scheme: 10 µl serum sample + 240 µl Sample Diluent

100 µl of distilled water was added to standard wells and sample wells. Standards were duplicated as described in the protocol. 50 µl of each 1:25 prediluted serum samples were added to the sample wells by mixing gently. Then, the plate was covered with an adhesive film and incubated at RT for 3 hours on a shaker at 400 rpm. After incubation, adhesive film was removed and supernatant in the wells was removed. 400 µl of Wash Buffer (provided by kit) per well was used to wash wells for six times. Each wash was allowed to sit in the wells for about 10-15 seconds before each aspiration of Wash Buffer. After washing was completed, plate was tapped on paper towel to remove remained Wash Buffer. 100 µl of TMB Substrate Solution was added to all wells and the plate was incubated at RT for 10 minutes in dark. 100 µl of Stop Solution provided by the kit was added to each well quickly. Then, the absorbance of each well was read right after the reaction was stopped by using a microplate reader at 450 nm and 620 nm. The absorbance of samples and standards were obtained. The standard curve was plotted and the concentration of sCD27 was calculated by following manufacture's instructions.

3.6. Statistical Analysis

Data were analyzed by using Chi-square, Student-t, Fisher's Exact, Man Whitney U, Kruskal Wallis tests with SPSS Version 17.0. Two-way ANOVA Test for Western blot data and ROC Curve analysis for ELISA results were performed in GraphPad Prism Version 8.2.1 For Windows.

4. RESULTS

4.1. Protein Expression by Western Blot

Tissue samples from 32 NSCLC patients were investigated by Western Blot and expression status of CD70, CD27, CD3, and FOXP3 molecules in the tumor microenvironment was revealed. Surgically removed primary tumor and adjacent normal tissue samples were individually analyzed. Table 4-1 shows the number of patients who are positive or negative for the expression of listed four molecules in the tumor microenvironment. CD70 expression was detected in only 5/32 (15.63%) tumor tissue samples, however, immunoblotting data showed that 24/32 (75%) tumor tissue samples have CD27 expression. In the tumor microenvironment, CD3 was observed in most of the patients (28/32), while only 14 patients had the expression of FOXP3.

Table 4-1: Number of positive or negative NSCLC patients for CD70, CD27, CD3, FOXP3 protein expression by Western Blot for only tumor tissue samples (n=32).

Molecules	Positive n (%)	Negative n (%)
CD70	5 (15.63%)	27 (84.37%)
CD27	24 (75%)	8 (25%)
CD3	28 (87.5%)	4 (12.5%)
FOXP3	14 (43.75%)	18 (56.25%)

A total of 32 patients were screened for immunoblotting. Surgically removed primary tumor and adjacent normal tissues from NSCLC patients were assessed. Actin was used as an internal loading control and bands were detected at 42 kDa. Measured data were analyzed in Image J 1.52a software and quantified bands were normalized according to Actin. Results were represented as relative densities in arbitrary units (a.u).

The positive control cell line (P3HR1) affirmed that CD70 expression was detected at around 65 kDa. Moreover, CD27 was spotted at 60 kDa and CD3 at 23 kDa. Lastly, FOXP3 expression was detected at approximately 50 kDa.

In the figures below (Figure 4-1 to Figure 4-8), expression analysis of quantified blots was represented. For each blot, a total of 4 patients and 8 samples were loaded to gels as indicated in the figures. Samples were arranged as tumor tissue sample of one patient and then the normal tissue sample of the same patient. Quantified data were analyzed in GraphPad Prism 8.2.1 and significance was calculated by two-way ANOVA test. Statistical analysis showed that differences between tumor and normal tissue expression were significant for all patients ($p<0.0001$).

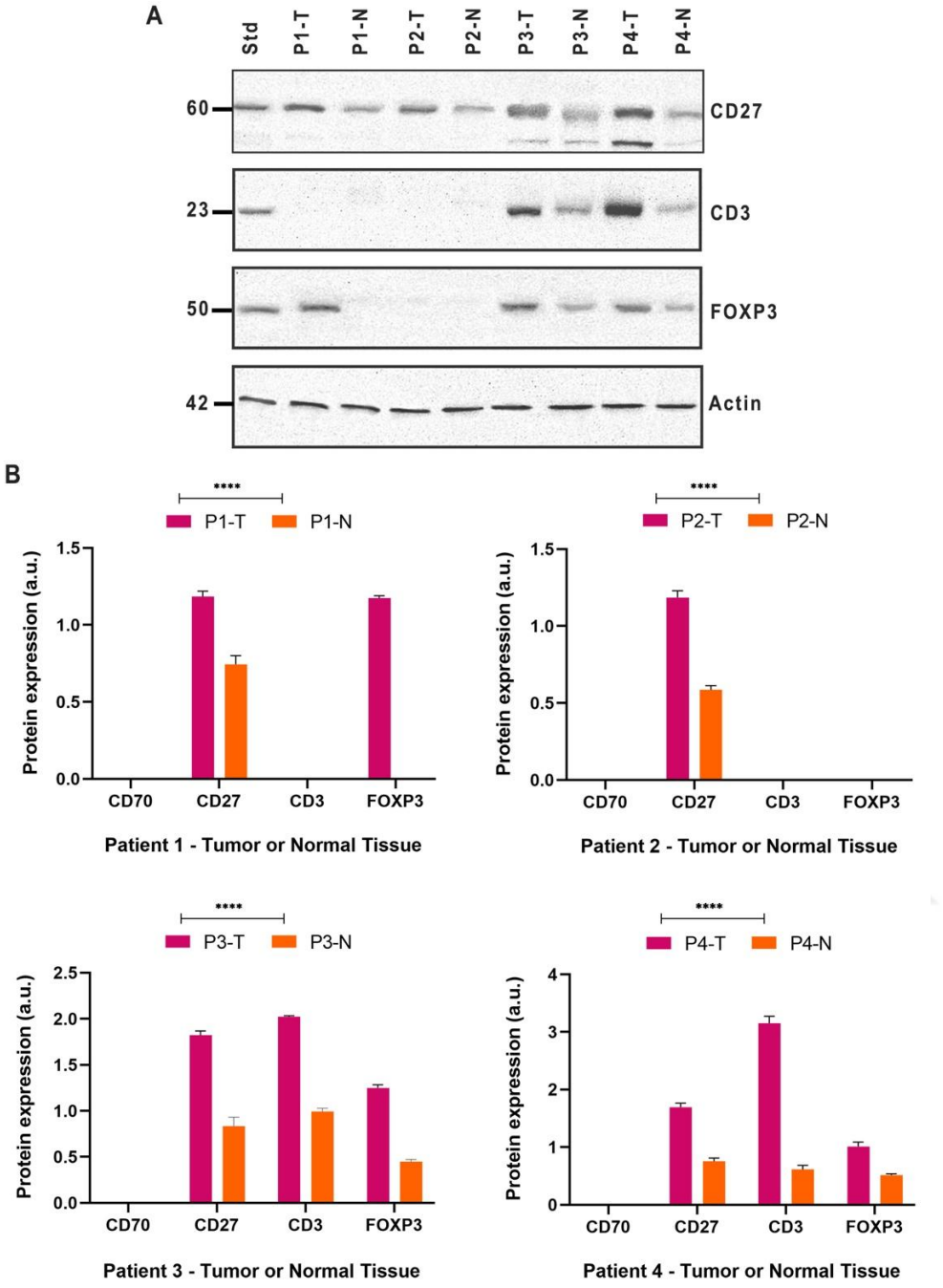

Figure 4-1: Expression of CD70, CD27, CD3, and FOXP3 molecules in the tumor microenvironment of 4 NSCLC patients (Patients 1-4). (A) Representative immunoblotting of CD27, CD3, and FOXP3 expression in NSCLC primary tumor tissues and normal adjacent tissues of Patient 1 (P1-T, P1-N), Patient 2 (P2-T, P2-N), Patient 3 (P3-T, P3-N), and Patient 4 (P4-T, P4-N). A standard sample was used for quantification and represented as Std. Actin was used as the loading control. **(B)** Quantified band intensities were indicated in the graphs in which protein expressions assessed in GraphPad Prism 8.2.0. Relative expression of tumor tissues was significantly higher than the normal tissues for all patients ($p<0.0001$). Error bars, SD (n=3). Protein expression level is represented in arbitrary units (a.u.).

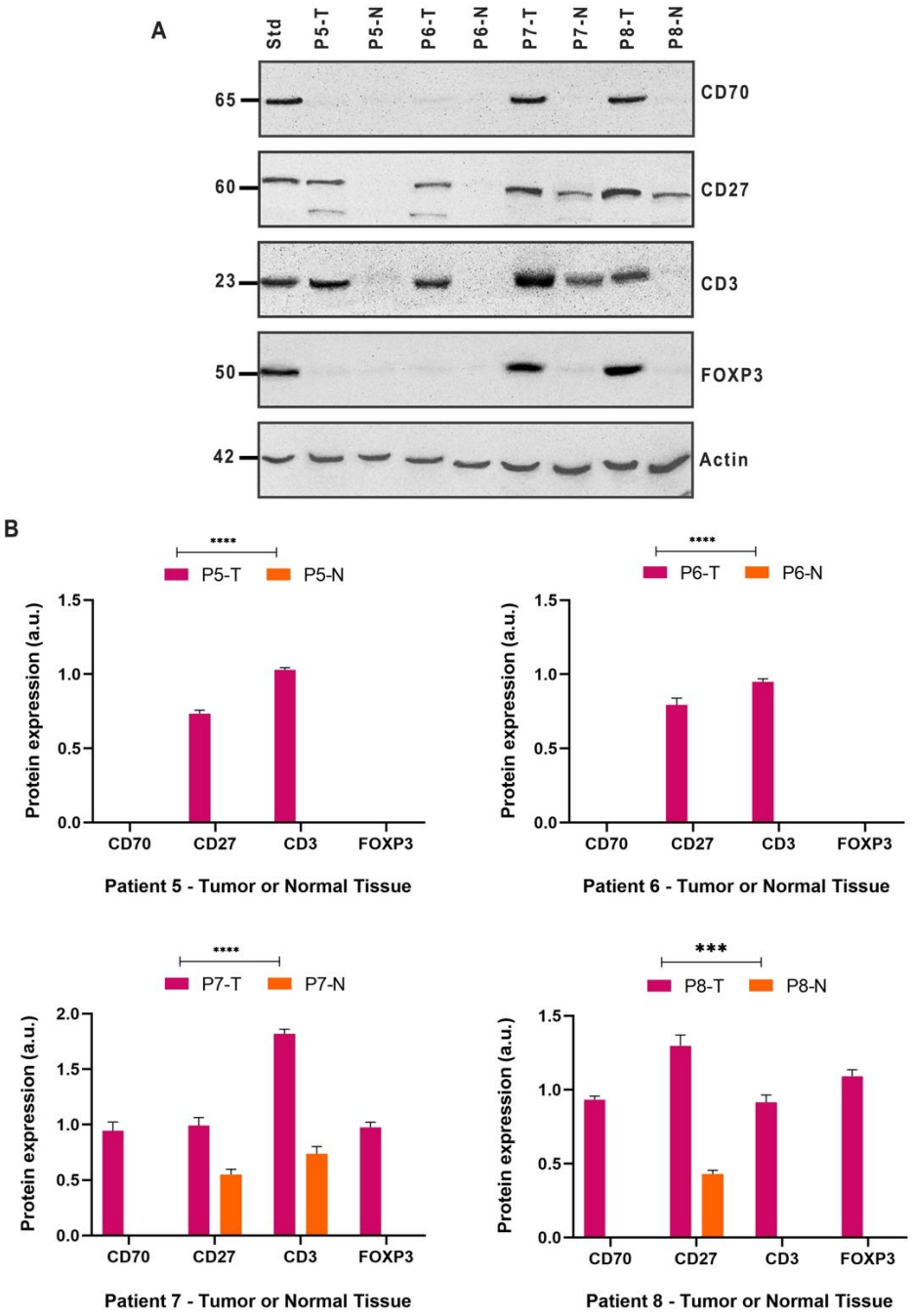

Figure 4-2: Expression of CD70, CD27, CD3, and FOXP3 molecules in the tumor microenvironment of 4 NSCLC patients (Patients 5-8). (A) Representative immunoblotting of CD27, CD3, and FOXP3 expression in NSCLC primary tumor tissues and normal adjacent tissues of Patient 5 (P5-T, P5-N), Patient 6 (P6-T, P6-N), Patient 7 (P7-T, P7-N), and Patient 8 (P8-T, P8-N). A standard sample was used for quantification and represented as Std. Actin was used as the loading control. **(B)** Quantified band intensities were indicated in the graphs in which protein expressions assessed in GraphPad Prism 8.2.0. Relative expression of tumor tissues was significantly higher than the normal tissues for all patients ($p<0.0001$). Error bars, SD (n=3). Protein expression level is represented in arbitrary units (a.u.).

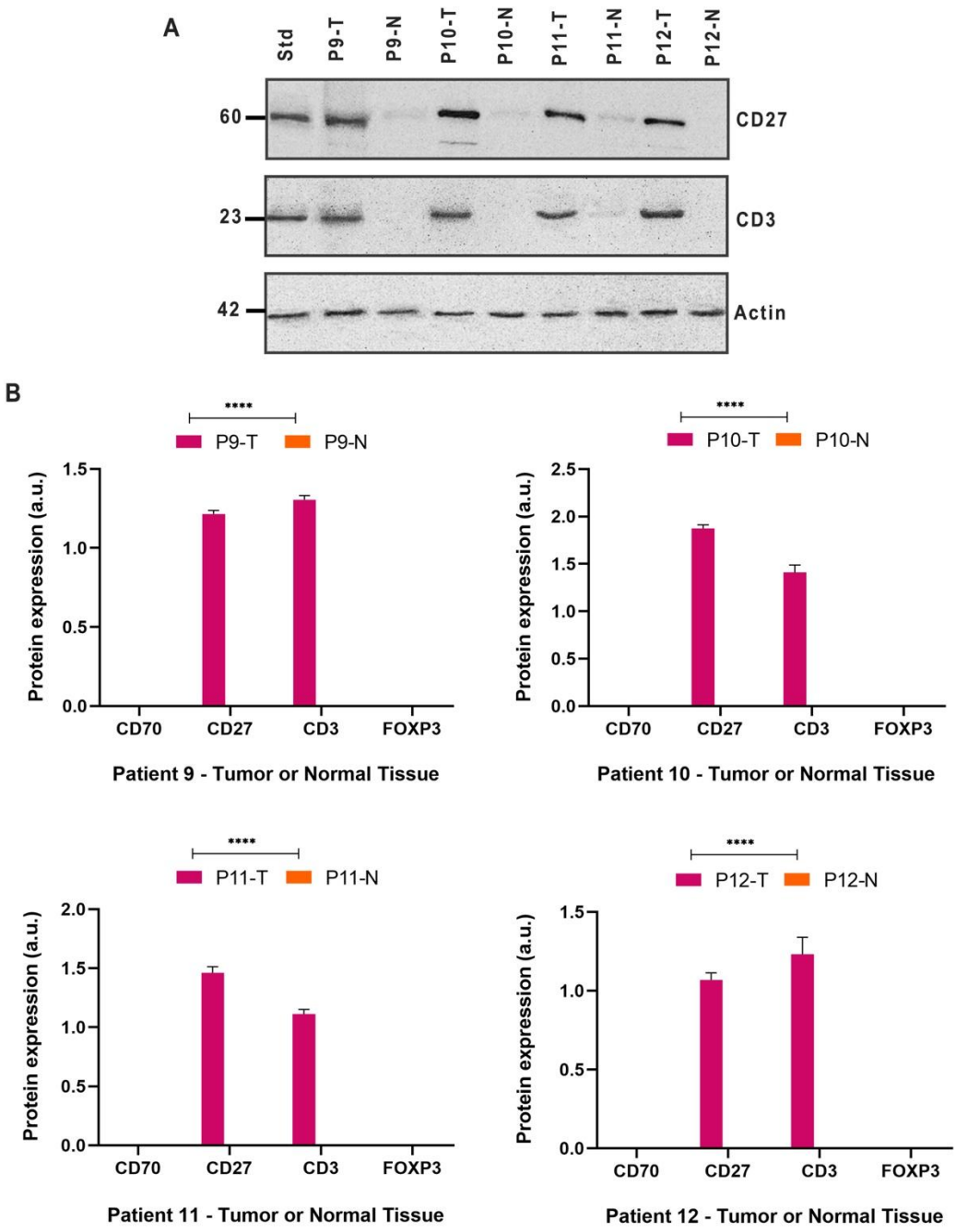

Figure 4-3: Expression of CD70, CD27, CD3, and FOXP3 molecules in the tumor microenvironment of 4 NSCLC patients (Patients 9-12). (A) Representative immunoblotting of CD27, CD3, and FOXP3 expression in NSCLC primary tumor tissues and normal adjacent tissues of Patient 9 (P9-T, P9-N), Patient 10 (P10-T, P10-N), Patient 11 (P11-T, P11-N), and Patient 12 (P12-T, P12-N). A standard sample was used for quantification and represented as Std. Actin was used as the loading control. **(B)** Quantified band intensities were indicated in the graphs in which protein expressions assessed in GraphPad Prism 8.2.0. Relative expression of tumor tissues was significantly higher than the normal tissues for all patients ($p<0.0001$). Error bars, SD (n=3). Protein expression level is represented in arbitrary units (a.u.).

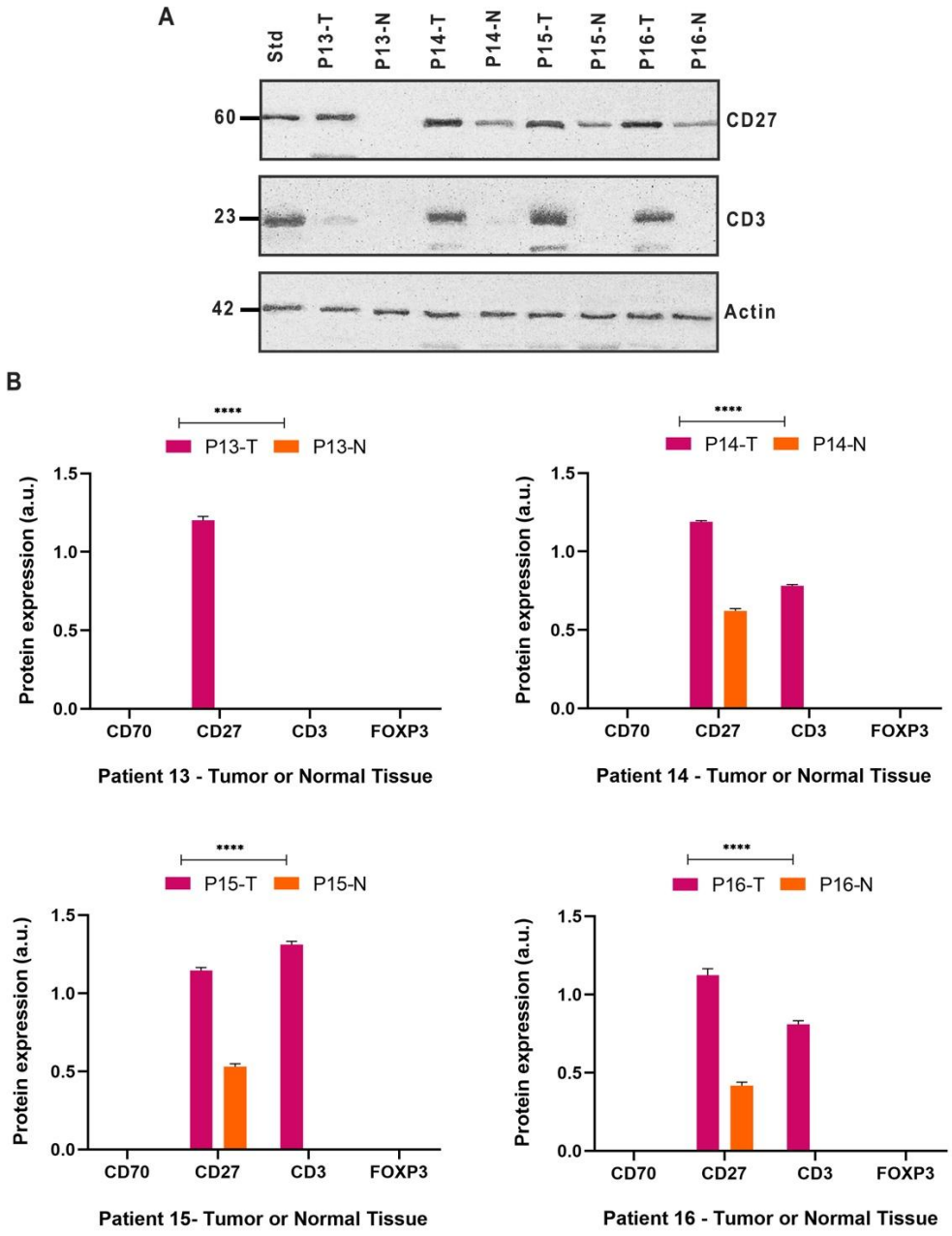

Figure 4-4: Expression of CD70, CD27, CD3, and FOXP3 molecules in the tumor microenvironment of 4 NSCLC patients (Patients 13-16). (A) Representative immunoblotting of CD27, CD3, and FOXP3 expression in NSCLC primary tumor tissues and normal adjacent tissues of Patient 13 (P13-T, P13-N), Patient 14 (P14-T, P14-N), Patient 15 (P15-T, P15-N), and Patient 16 (P16-T, P16-N). A standard sample was used for quantification and represented as Std. Actin was used as the loading control. **(B)** Quantified band intensities were indicated in the graphs in which protein expressions assessed in GraphPad Prism 8.2.0. Relative expression of tumor tissues was significantly higher than the normal tissues for all patients ($p<0.0001$). Error bars, SD (n=3). Protein expression level is represented in arbitrary units (a.u.).

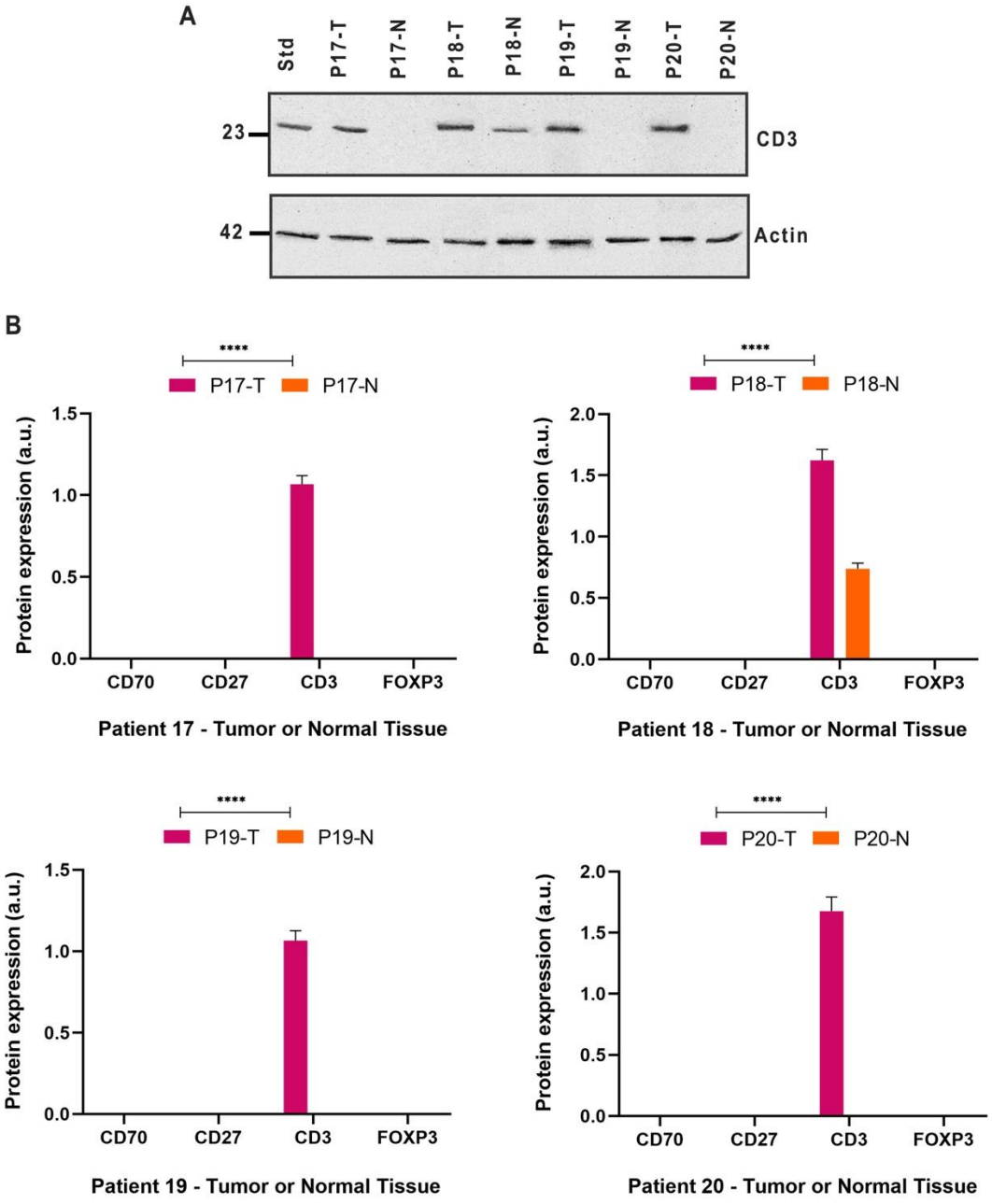

Figure 4-5: Expression of CD70, CD27, CD3, and FOXP3 molecules in the tumor microenvironment of 4 NSCLC patients (Patients 17-20). (A) Representative immunoblotting of CD27, CD3, and FOXP3 expression in NSCLC primary tumor tissues and normal adjacent tissues of Patient 17 (P17-T, P17-N), Patient 18 (P18-T, P18-N), Patient 19 (P19-T, P19-N), and Patient 20 (P20-T, P20-N). A standard sample was used for quantification and represented as Std. Actin was used as the loading control. **(B)** Quantified band intensities were indicated in the graphs in which protein expressions assessed in GraphPad Prism 8.2.0. Relative expression of tumor tissues was significantly higher than the normal tissues for all patients ($p<0.0001$). Error bars, SD (n=3). Protein expression level is represented in arbitrary units (a.u.).

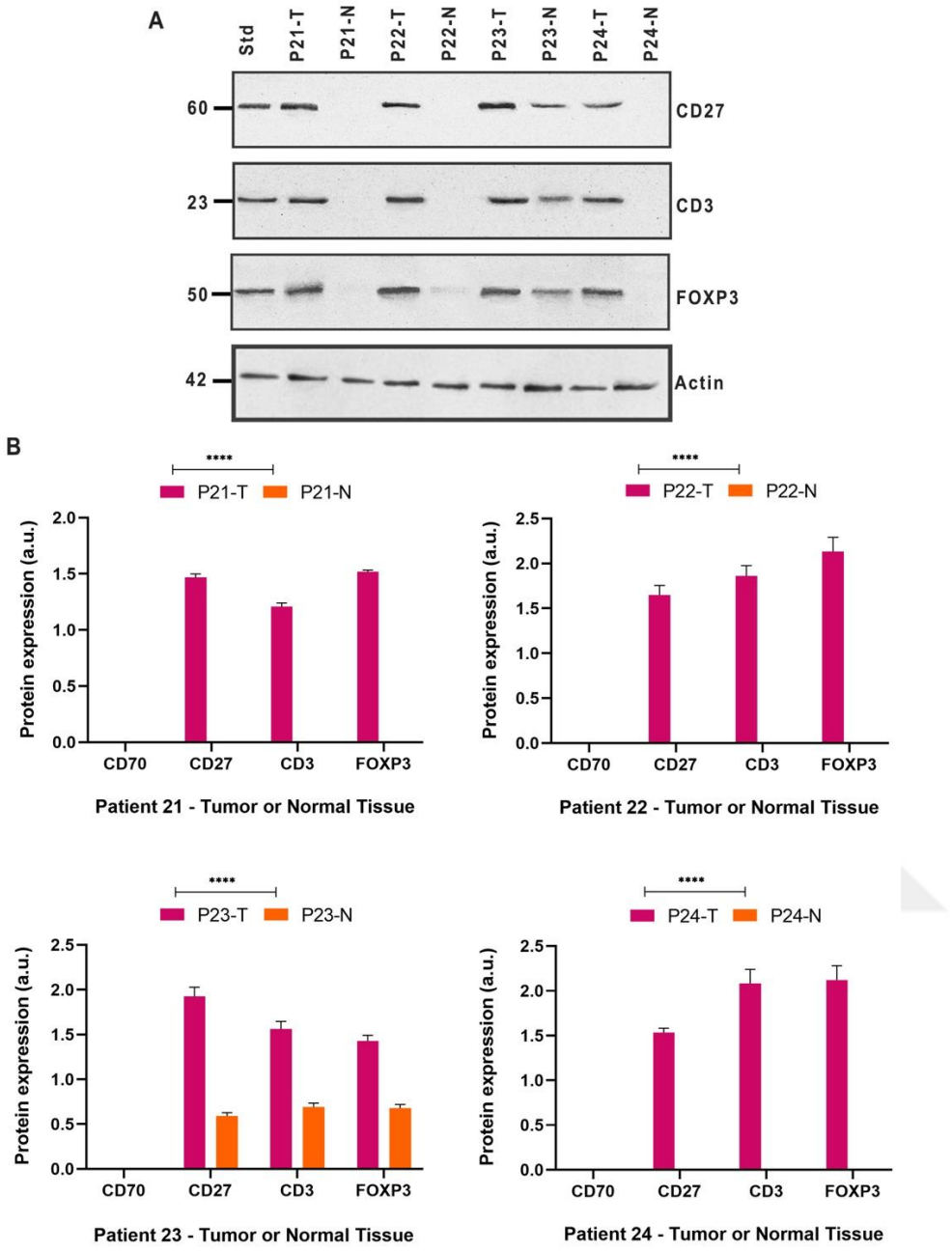

Figure 4-6: Expression of CD70, CD27, CD3, and FOXP3 molecules in the tumor microenvironment of 4 NSCLC patients (Patients 21-24). (A) Representative immunoblotting of CD27, CD3, and FOXP3 expression in NSCLC primary tumor tissues and normal adjacent tissues of Patient 21 (P21-T, P21-N), Patient 22 (P22-T, P22-N), Patient 23 (P23-T, P23-N), and Patient 24 (P24-T, P24-N). A standard sample was used for quantification and represented as Std. Actin was used as the loading control. **(B)** Quantified band intensities were indicated in the graphs in which protein expressions assessed in GraphPad Prism 8.2.0. Relative expression of tumor tissues was significantly higher than the normal tissues for all patients ($p<0.0001$). Error bars, SD (n=3). Protein expression level is represented in arbitrary units (a.u.).

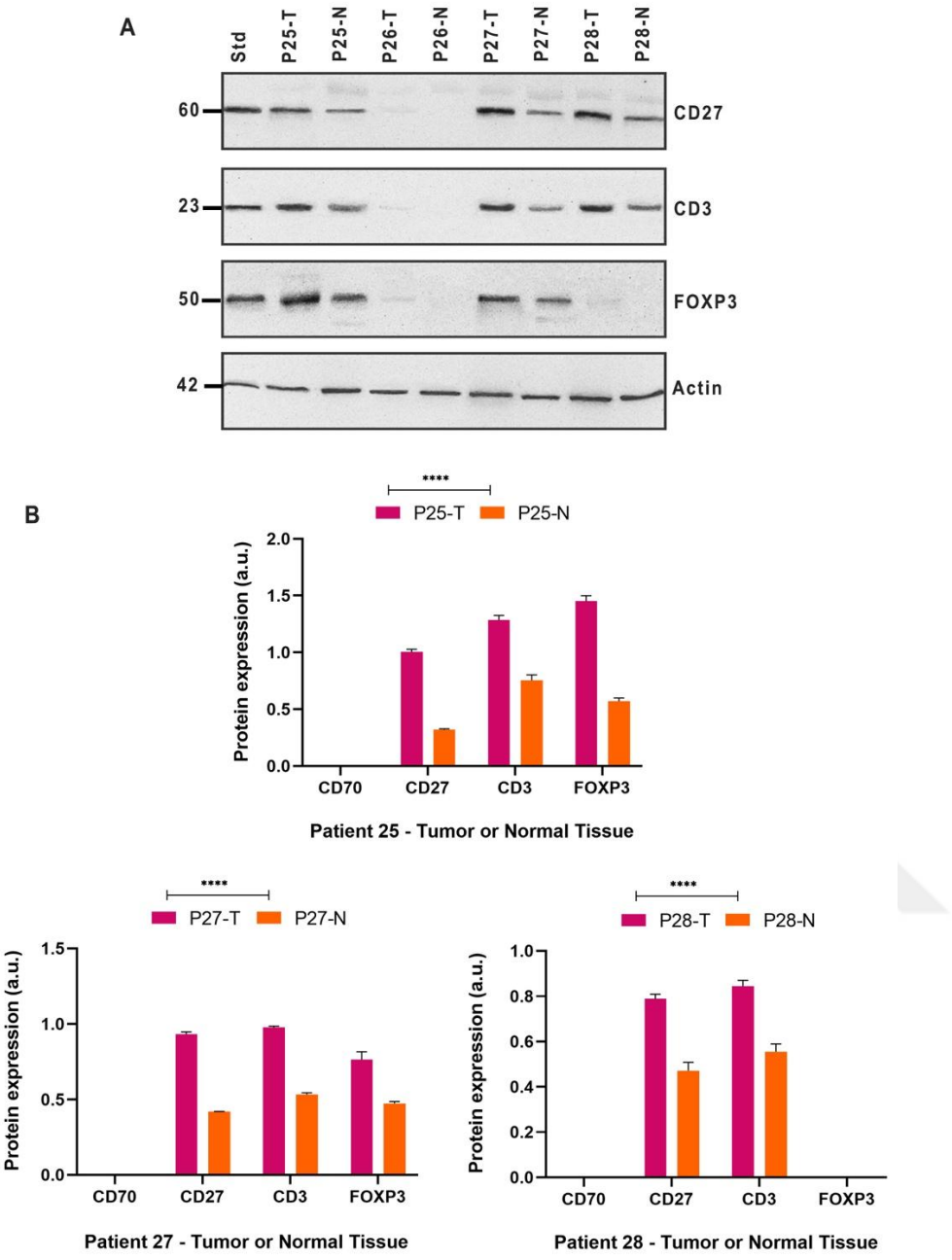

Figure 4-7: Expression of CD70, CD27, CD3, and FOXP3 molecules in the tumor microenvironment of 4 NSCLC patients (Patients 25-28). (A) Representative immunoblotting of CD27, CD3, and FOXP3 expression in NSCLC primary tumor tissues and normal adjacent tissues of Patient 25 (P25-T, P25-N), Patient 26 (P26-T, P26-N), Patient 27 (P27-T, P27-N), and Patient 28 (P28-T, P28-N). A standard sample was used for quantification and represented as Std. Actin was used as a loading control. **(B)** Quantified band intensities were indicated in the graphs in which protein expressions assessed in GraphPad Prism 8.2.0. Relative expression of tumor tissues was significantly higher than the normal tissues for all patients ($p<0.0001$). Error bars, SD (n=3). Protein expression level is represented in arbitrary units (a.u.).

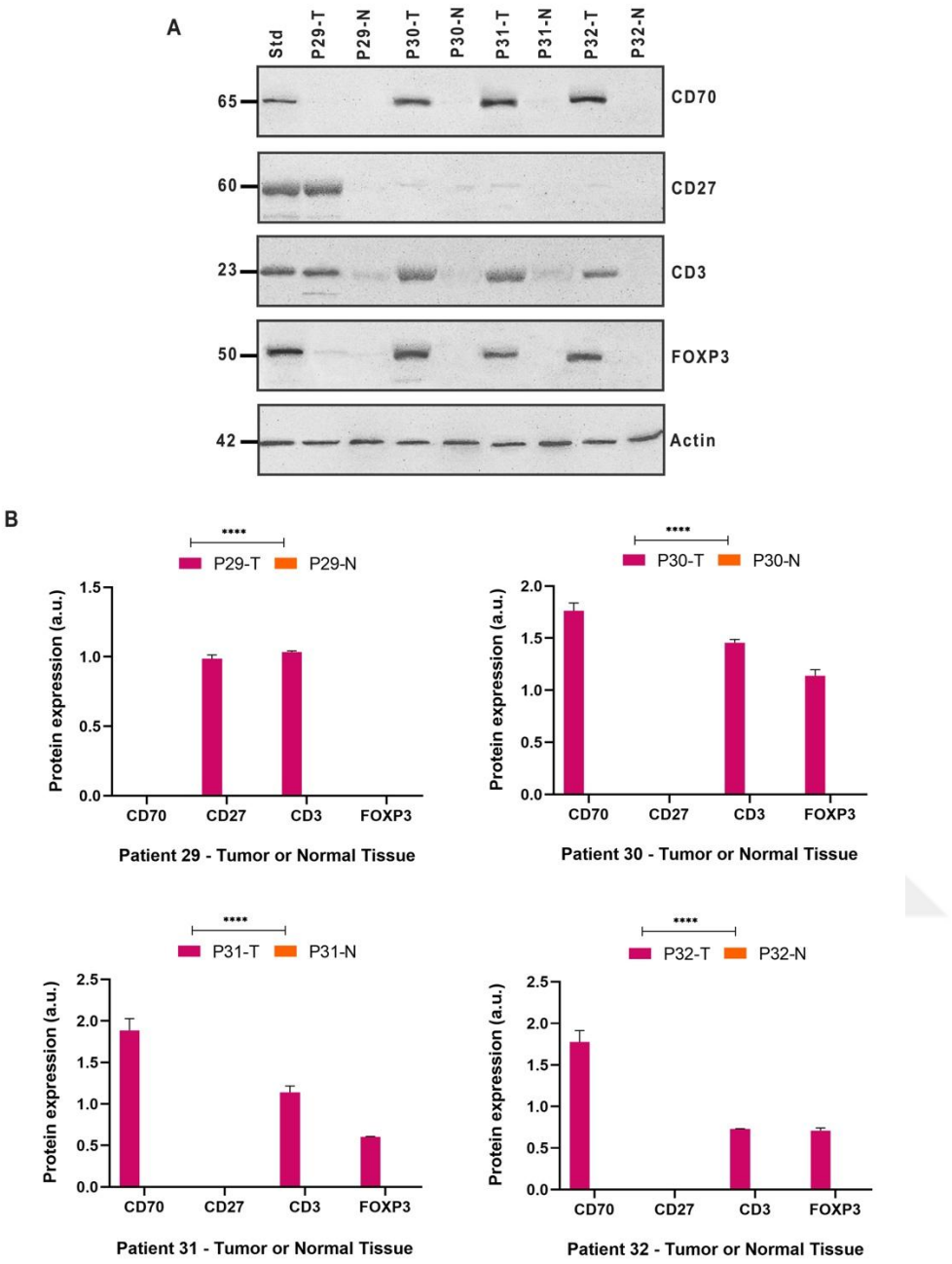

Figure 4-8: Expression of CD70, CD27, CD3, and FOXP3 molecules in the tumor microenvironment of 4 NSCLC patients (Patients 29-32). (A) Representative immunoblotting of CD27, CD3, and FOXP3 expression in NSCLC primary tumor tissues and normal adjacent tissues of Patient 29 (P29-T, P29-N), Patient 30 (P30-T, P30-N), Patient 31 (P31-T, P31-N), and Patient 32 (P32-T, P32-N). A standard sample was used for quantification and represented as Std. Actin was used as a loading control. **(B)** Quantified band intensities were indicated in the graphs in which protein expressions assessed in GraphPad Prism 8.2.0. Relative expression of tumor tissues was significantly higher than the normal tissues for all patients ($p<0.0001$). Error bars, SD (n=3). Protein expression level is represented in arbitrary units (a.u.).

4.2. Demographic Distribution And Clinicopathological Characteristics Of The Study Group

The study group contains 45 patients and 32 healthy subjects in total. Expression analysis by Western Blot was performed for 32 patients while 16 of those patients were also screened by ELISA to measure sCD27 serum level. Serum levels of sCD27 were measured for 30 patients in total. Age and gender distribution for the study group are shown in Table 4-2.

Table 4-2: Age and gender parameters for the study group.

Parameters	NSCLC Patients n=46 (%)	Healthy Controls n=32 (%)	p
Age (years) Mean ± SD	58.72 ± 9.33	50.87 ± 1.97	0.078
Gender			
Female	9 (20%)	7 (21.9%)	0.711
Male	37 (80%)	25 (78.1%)	

The classification of NSCLC patients in the study group was performed based on patients' clinicopathological characteristics. Table 4-3 shows the number of patients and percentages for each parameter.

Table 4-3: Clinicopathological features of NSCLC patients in the study group.

Parameters	NSCLC Patients n (%)
Histological Type	
Adenocarcinoma	11 (37.9%)
Squamous cell	14 (48.3%)
Large cell	2 (6.9%)
Other	2 (6.9%)
Tumor Stage	
T1	11 (37.9%)
T2	9 (31%)
T3	9 (31%)

Lymph node metastasis	
N0	19 (65.5%)
N1	10 (34.5%)
Distant organ metastasis	
Yes	1 (3.4%)
No	28 (96.6%)
Perineural invasion	
Yes	15 (51.7%)
No	14 (48.3%)
Angiolymphatic invasion	
Yes	25 (86.2%)
No	4 (13.8%)
Vascular invasion	
Yes	13 (46.4%)
No	15 (53.6%)
Smoking	
Yes	29 (100%)
No	—

Clinicopathological characteristics of patients were then correlated with the expression status of CD70, CD27, CD3, and FOXP3 molecules (Table 4-4). No significant correlation was found between the expression status and clinicopathological characteristics of patients.

Table 4-4: Correlation between clinicopathological characteristics of patients and protein expression status of CD70, CD27, CD3, and FOXP3 in the tumor microenvironment of NSCLC patients.

Parameters	**CD70 n (%)**		**CD27 n (%)**		**CD3 n (%)**		**FOXP3 n (%)**	
	positive	**negative**	**positive**	**negative**	**positive**	**negative**	**positive**	**negative**
Tumor Stage								
T1 +T2	5 (55.6)	4 (44.4%)	4 (44.4%)	5 (55.6%)	8 (88.9%)	1 (11.1%)	5 (55.6%)	4 (44.4%)

T3 +T4	1 (12.5%)	7 (87.5%)	5 (62.5%)	3 (18.8%)	6 (75%)	2 (25%)	4 (50%)	4 (50%)
	p=0.131		p=0.637		p=0.576		p=1.00	
Lymph node metastasis								
N0	3 (37.5%)	5 (62.5%)	4 (50%)	4 (50%)	6 (75%)	2 (25%)	5 (62.5%)	3 (37.5%)
N1, N2, N3	3 (33.3%)	6 (66.7%)	5 (55.6%)	4 (44.4%)	8 (88.9%)	1 (11.1%))	4 (44.4%)	5 (55.6%)
	p=1.00		p=1.00		p=0.576		p=0.637	
Distant organ metastatis								
Yes	1 (100%)	—	—	1 (100%)	1 (100%)	—	1 (100%)	—
No	5 (31.2%)	11 (68.8%)	9 (56.2%)	7 (43.8%)	13 (81.2%)	3 (18.8%)	8 (50%)	8 (50%)
	p=0.353		p=0.471		p=1.00		p=1.00	
Perineural invasion								
Yes	4 (40%)	6 (60%)	7 (70%)	3 (30%)	8 (80%)	2 (20%)	6 (60%)	4 (40%)
No	2 (28.6%)	5 (72.4%)	2 (28.6%)	5 (71.4%)	6 (85.7%)	1 (14.3%)	3 (42.9%)	4 (57.1%)
	p=1.00		p=0.153		p=1.00		p=0.637	
Angiolymphatic invasion								
Var	5 (35.7%)	9 (64.3%)	9 (64.3%)	5 (35.7%)	12 (85.7%)	2 (14.3%)	8 (57.1%)	6 (42.9%)
Yok	1 (33.3)	2 (66.7%)	—	3 (100%)	2 (66.7%)	1 (33.3%)	1 (33.3%)	2 (66.7%)
	p=1.00		**p=0.082**		p=0.465		p=0.576	
Vascular invasion								
Yes	1 (20%)	4 (80%)	3 (60%)	2 (40%)	4 (80%)	1 (20%)	2 (40%)	3 (60%)

No	4 (36.4%)	17 (63.6%)	6 (54.5%)	5 (45.5%)	9 (81.2%)	2 (18.2%)	6 (54.5%)	5 (45.5%)
	p=1		p=1		p=1		p=1	

4.3. Detection Of sCD27 Level On Patients Sera of NSCLC Patients

Serum samples of 30 NSCLC patients and 32 healthy controls were collected to measure sCD27 serum levels. Table 4-5 shows that the mean level (mean±SD) of sCD27for NSCLC patients is 117.29 ± 38.18 U/ml with a range of 50.24-236.49 U/ml.

Table 4-5: Measured sCD27 serum levels of NSCLC patients and healthy controls. SPSS Version 17.0 software was used to analyze the data (p<0.0001).

Parameters	**NSCLC Patients n=30 (mean ± SD)**	**Healthy Controls n=32 (mean ± SD)**	**p**
sCD27 U/ml	117.29 ± 38.18	82.38 ± 21.99	p<0.0001

The cut-off value was set as 88.91 U/ml by ROC analysis for sCD27. Additionally, sensitivity was detected as 0.90 and specificity was identified as 0.72 (Figure 4-9).

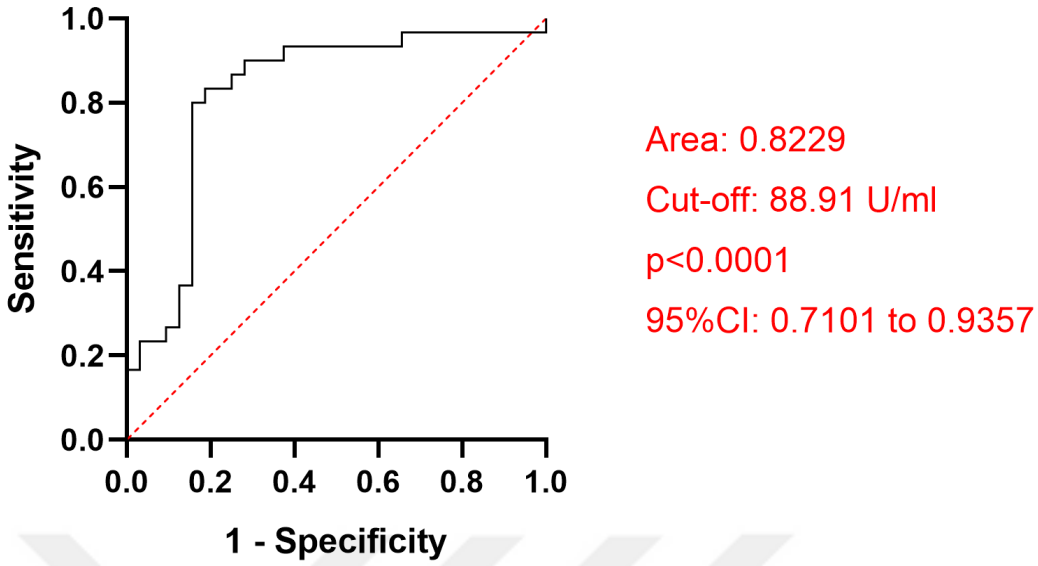

Figure 4-9: Sensitivity and specificity were determined by ROC Curve analysis for sCD27 levels of NSCLC patients and healthy controls. sCD27 levels were counted as positive for the values above 88.91 U/ml, the patient group has the sensitivity of 90% and specificity of 72% ($p<0.0001$). ROC Curve analysis was carried out by GraphPad Prism 8.2.1.

ELISA results showed high sensitivity and specificity, that the test correctly identifies the high sCD27 levels-patients with strong significance ($p<0.0001$).

Measured sCD27 serum levels were correlated with patients' clinicopathological characteristics and no correlation was found with sCD27 levels and the parameters shown in Table 4-6.

Table 4-6: Correlation between clinicopathological features of NSCLC patients and serum sCD27 levels. The correlation was calculated in the SPSS Version 17.0 software.

Parameters	sCD27 level (U/ml) (mean ± SD)	p
Tumor Stage		
T1 +T2	117.86 ± 32.14	0.804
T3 +T4	119.7 ± 49.89	

Lymph node metastasis		
N0	122.64 ± 45.98	0.804
N1, N2, N3	110.63 ± 14.96	
Distant organ metastasis		
Yes	208.86	1.00
No	115.27 ± 34.72	
Perineural invasion		
Yes	125.28 ± 50.24	0.591
No	111.23 ± 18.06	
Angiolymphatic invasion		
Yes	121.52 ± 40.42	0.160
No	99.62 ± 6.91	
Vascular invasion		
Yes	120.01 ± 43.76	0.928
No	118.39 ± 35.53	

High serum level of sCD27 was found to be correlated with CD70 positivity on tumor microenvironment of NSCLC patients (p=0.007). Although CD27 and FOXP3 did not correlate to the sCD27 level, CD3 correlation was close to a significant value (p=0.091) (Table 4-7).

Table 4-7: Relation between sCD27 serum levels and expression status of CD70, CD27, CD3, and FOXP3 in the tumor microenvironment of NSCLC patients. Correlation analysis was performed in the SPSS Version 17.0 software.

Parameters	Expression status		p
sCD27 U/ml	**CD70 (mean ± SD)**		
	Positive (n=5)	**Negative (n=11)**	**0.007**
	155.96 ± 54.48	95.79 ± 19.87	
	CD27 (mean ± SD)		
	Positive (n=16)	**Negative (n=5)**	0.423
	101.70 ± 29.1	134.28 ± 55.57	
	CD3 (mean ± SD)		
	Positive (n=16)	**Negative (n=5)**	0.091
	124.60 ± 45.34	81.70 ± 28.05	
	FOXP3 (mean ± SD)		
	Positive (n=12)	**Negative (n=9)**	0.423
	132.35 ± 55.92	99.79 ± 21.85	

According to the ROC Curve analysis, the cutoff value was 88.91 U/ml for the sCD27 level. The number of patients who are positive or negative for sCD27 serum level was correlated to clinicopathological characteristics or expression status (Table 4-8). No correlation was found.

Table 4-8: Relation between sCD27 serum levels and clinicopathological characteristics or expression status of CD70, CD27, CD3, and FOXP3 in the tumor microenvironment of NSCLC patients. The patients with higher sCD27 serum levels than the cutoff value, 88.91 U/ml, considered as positive and patients with lower serum levels than 88.91 U/ml taken as negative.

Parameters	sCD27 level (U/ml) n (%)		
	Positive	**Negative**	**p**
Gender			
Male	16 (80.15%)	4 (20%)	0.328
Female	4 (57.1%)	3 (42.9%)	
Tumor stage			
T1+T2	19 (100%)	—	0.111
T3+T4	8 (80%)	2 (20%)	
Lymph node metastasis			
N0	17 (89.5%)	2 (10.5%)	0.532
N1+N2+N3	10 (100%)	—	
Distant organ metastasis			
Yes	1 (100%)	—	1.00
No	26 (92.9%)	2 (7.1%)	
Perineural invasion			
Yes	13 (86.7%)	2 (13.3%)	0.483
No	14 (100%)	—	
Angiolymphatic invasion			
Yes	23 (92.0%)	2 (8.0%)	1.00
No	4 (100%)	—	
Vascular invasion			

Yes	11 (84.6%)	2 (15.4%)	0.206
No	15 (100%)	—	
CD70 expression			
Yes	5 (100%)	—	0.515
No	9 (81.8%)	2 (18.2%)	
CD27 expression			
Yes	7 (77.8%)	2 (22.2%)	0.471
No	8 (100%)	—	
CD3 expression			
Yes	13 (92.9%)	1 (7.1%)	0.331
No	2 (66.7%)	1 (33.3%)	
FOXP3 expression			
Yes	8 (88.9%)	1 (11.1%)	1.00
No	7 (87.5%)	1 (12.5%)	

5. DISCUSSION

Lung cancer has the highest incidence in the world and NSCLC consists of 85% of all cases. It is important that there are precise biomarkers that allow detection and diagnosis of the disease for correct evaluation of the patient characteristics. CD70 has been shown that it is a very promising target as a potential biomarker for NSCLC. [55]

In this study, the expression profile of CD70, CD27, CD3, and FOXP3 molecules were investigated in 32 NSCLC tumors and adjacent normal tissues. Also, sCD27 level was detected in 30 NSCLC patient sera. Data were evaluated with clinicopathological characteristics of the patient group.

CD70 is one of the immune checkpoint molecules and found on activated T cells and B cells, and DCs in normal conditions. Since its expression is always under very tight control, unregular tumor expression of CD70 causes aberrant activation of TILs and other immune cells in TME resulting immune suppression. Furthermore, it is shown that there is no CD70 expression on normal tissue but CD70 expression on some solid tumors and hematologic malignancies have been found. Renal cell carcinoma is characterized as strong positive for CD70, as well as glioblastoma showed CD70 overexpression profile. Many other types of cancer have been also screening in order to evaluate potential usages of CD70 as a biomarker for patient outcomes and prognosis such as ovarian cancer, colorectal cancer, breast cancer, and NSCLC. NSCLC is among those types of cancer but there are only few studies that show CD70 related mechanisms. Thus, further investigation is necessary. [8], [55]–[60]

CD70 is the ligand of the CD27 receptor which is expressed only on immune cells such as T cells, B cells, and NK cells. No tumor or normal tissue expression has been shown for CD27. Normally, CD27 has a costimulatory effect on immune cells through the interaction of its ligand, CD70. It is responsible for proliferation of T cells, differentiation of memory T cells, and proper activation of T cells, and also differentiation of plasma cells, maturation of B cells with CD70/CD27 signaling pathway. However, CD70-CD27 related mechanisms cause immune evasion when overexpression of CD70 is seen in the TME. Promoting T cell apoptosis and accumulation of Tregs in TME are involved as a result of this mechanism. Also, once CD27 binds to CD70, cleaving of CD27 from TILs have been occurred and the cleaved

molecule is released to the serum as a soluble CD27 (sCD27) form. Some studies revealed that sCD27 level is correlated with patient clinicopathological features. [8], [55]–[62]

Interaction between CD27 and CD70 leads to Treg accumulation on TME. FOXP3 is known as a Treg marker and FOXP3+ Tregs are related to immune suppression. Furthermore, Treg accumulation in TME is also found to be correlated with poor outcome of the patients' clinical characteristics. On the other hand, CD3 is T cell biomarker and CD3 positivity in TME tells that there is a T cell accumulation in the TME. Types and locations of T cells in the TME is important factor for future of the tumor because T cells can directly kill tumors. Therefore, FOXP3 and CD3 expression were investigated to check whether FOXP3+ and CD3+ immune cell accumulation are correlated with immune checkpoint molecules, CD70/CD27, and their mechanisms. [5], [55], [56], [63], [64]

In this study, CD70 expression was detected for only 5/32 (15.63%) of NSCLC tissues and none of their adjacent normal tissues showed CD70 positivity by Western Blot as expected. Thus, NSCLC is not among tumors in which CD70 is overexpressed in the majority of the tumor. Additionally, Jacobs et al., 2015 showed that only 16.3% of the tissues which are investigated by immunohistochemistry (IHC) were positive for CD70 in NSCLC. Also, it was not found any correlation between histological types or any other clinicopathological features of patients for CD70 positivity. FOXP3 and CD3 showed same pattern of expressions with CD70 in tumor tissues. This finding for tissues that showed CD70 expression also had FOXP3 and CD3 expressions support previous studies that state expression of CD70 in TME comes with FOXP3+ Treg and CD3+ T cell accumulations. However, it requires more patients in order to make a reliable conclusion for their relationship in TME because only 5 tissues out of 33 showed CD70 positivity. Thus, higher number of patients are needed to be screen with a technique that allows seeing the locations of the expression of molecules such as immunohistochemistry. [8], [55]–[62]

In normal conditions, CD70 expression on Western Blot needed to be detected at 21 kDa according to the antibody instructions. However, in this study, CD70 was detected at 65 kDa for positive control cell lines and tumor tissues. A study was shown that by Jilaveanu et al, 2012, monomer (20.9 kDa), dimer (42 kDa), and trimer (63 kDa)

forms were detected by Western Blot with highly specific anti-CD70 antibody. Therefore, trimeric form of CD70 was detected in this study. [58]

Overall 22 patients out of 32 showed the exact same pattern of expression for CD27 and CD3 in this study. Ruf et al, 2015, showed CD27+ TILs in TME are actually CD3+ T cells. Although same pattern of expression supports this finding, it does not exactly say the source of expression.

sCD27 level was detected for 30 NSCLC patients and 32 healthy controls. The level of sCD27 was found statistically significant ($p<0.0001$) for the patient group with very high sensitivity (90%) suggesting that sCD27 has a potential usage as a diagnostic biomarker for NSCLC for detection of the disease. However, there was no significant correlation found between clinicopathological features of the patients and sCD27 level. Thus, sCD27 can not predict patient outcome over the disease. [8], [55], [57]

sCD27 level was also assessed with the expression status of CD70, CD27, CD3 and FOXP3 molecules in NSCLC. CD70 positivity on tumor tissues was found to be significantly correlated with the level of sCD27 ($p=0.007$) in serum with respect to CD70 negativity supporting that CD70/CD27 interaction in TME causes the cleaving off CD27 and increasing the level of sCD27 in patient sera. On the other hand, there was no significant result between CD27 and FOXP3 positivity and sCD27 level. Moreover, higher level of sCD27 showed relatively significant results for CD3 positivity ($p=0.091$) which supports previous studies where higher CD3 accumulation in TME was found to be correlated with patients with higher levels of sCD27 in patient sera. [8], [55], [57]

The molecular biology technique that was used in this study, Western Blot, for detection of expression of molecules came with several disadvantages. It does not allow us to detect the locations of proteins in TME. Thus, further investigation is necessary to detect the localization and the source of CD70, CD27, FOXP3, and CD3 positivity in NSCLC with higher number of patients.

REFERENCES

[1] F. Bray, J. Ferlay, I. Soerjomataram, R. L. Siegel, L. A. Torre, and A. Jemal, "Global cancer statistics 2018: GLOBOCAN estimates of incidence and mortality worldwide for 36 cancers in 185 countries," *CA. Cancer J. Clin.*, vol. 68, no. 6, pp. 394–424, 2018.

[2] World Health Organisation, "Latest global cancer data: Cancer burden rises to 18.1 million new cases and 9.6 million cancer deaths in 2018," *Int. Agency Res. cancer*, no. September, pp. 13–15, 2018.

[3] J. A. Barta, C. A. Powell, and J. P. Wisnivesky, "Global Epidemiology of Lung Cancer," *Ann. Glob. Heal.*, vol. 85, no. 1, pp. 1–16, 2019.

[4] N. Duma, R. Santana-Davila, and J. R. Molina, "Non–Small Cell Lung Cancer: Epidemiology, Screening, Diagnosis, and Treatment," *Mayo Clin. Proc.*, vol. 94, no. 8, pp. 1623–1640, 2019.

[5] B. Stankovic *et al.*, "Immune Cell Composition in Human Non-small Cell Lung Cancer," *Front. Immunol.*, vol. 9, no. February, p. 3101, 2018.

[6] S. L. Buchan, A. Rogel, and A. Al-Shamkhani, "The immunobiology of CD27 and OX40 and their potential as targets for cancer immunotherapy," *Blood*, vol. 131, no. 1. American Society of Hematology, pp. 39–48, 04-Jan-2018.

[7] I. S. Grewal, "CD70 as a therapeutic target in human malignancies," *Expert Opinion on Therapeutic Targets*, vol. 12, no. 3. pp. 341–351, Mar-2008.

[8] M. Ruf, H. Moch, and P. Schraml, "Interaction of tumor cells with infiltrating lymphocytes via CD70 and CD27 in clear cell renal cell carcinoma," *Oncoimmunology*, vol. 4, no. 12, Dec. 2015.

[9] D. R. Shaffer *et al.*, "T cells redirected against CD70 for the immunotherapy of CD70-positive malignancies," *Blood*, vol. 117, no. 16, pp. 4304–4314, Apr. 2011.

[10] J. Ferlay *et al.*, "Estimating the global cancer incidence and mortality in 2018: GLOBOCAN sources and methods," *Int. J. Cancer*, vol. 144, no. 8, pp. 1941–1953, 2019.

[11] K. Inamura, "Lung cancer: understanding its molecular pathology and the 2015 WHO classification," *Front. Oncol.*, vol. 7, no. AUG, pp. 1–7, 2017.

[12] S. Wang, S. Zimmermann, K. Parikh, A. S. Mansfield, and A. A. Adjei, "Current

Diagnosis and Management of Small-Cell Lung Cancer," *Mayo Clin. Proc.*, vol. 94, no. 8, pp. 1599–1622, 2019.

[13] S. L. Wood, M. Pernemalm, P. A. Crosbie, and A. D. Whetton, "The role of the tumor-microenvironment in lung cancer-metastasis and its relationship to potential therapeutic targets," *Cancer Treat. Rev.*, vol. 40, no. 4, pp. 558–566, 2014.

[14] "What Is Non-Small Cell Lung Cancer?" [Online]. Available: https://www.cancer.org/cancer/non-small-cell-lung-cancer/about/what-is-non-small-cell-lung-cancer.html. [Accessed: 20-Aug-2019].

[15] "Can Non-Small Cell Lung Cancer Be Found Early?" [Online]. Available: https://www.cancer.org/cancer/non-small-cell-lung-cancer/detection-diagnosis-staging/detection.html. [Accessed: 21-Aug-2019].

[16] S. B. Knight, P. A. Crosbie, H. Balata, J. Chudziak, T. Hussell, and C. Dive, "Progress and prospects of early detection in lung cancer," *Open Biol.*, vol. 7, no. 9, 2017.

[17] A. S. Berghoff *et al.*, "Immune checkpoint inhibitor treatment in patients with oncogene- addicted non-small cell lung cancer (NSCLC): Summary of a multidisciplinary round-table discussion," *ESMO Open*, vol. 4, no. 3, pp. 1–12, 2019.

[18] U. Testa, G. Castelli, and E. Pelosi, "Lung cancers: Molecular characterization, clonal heterogeneity and evolution, and cancer stem cells," *Cancers (Basel).*, vol. 10, no. 8, pp. 1–81, 2018.

[19] M. Majem *et al.*, "Multidisciplinary consensus statement on the clinical management of patients with stage III non-small cell lung cancer," *Clin. Transl. Oncol.*, no. 0123456789, 2019.

[20] "Non-Small Cell Lung Cancer Stages." [Online]. Available: https://www.cancer.org/cancer/non-small-cell-lung-cancer/detection-diagnosis-staging/staging.html. [Accessed: 22-Aug-2019].

[21] M. Dietel *et al.*, "Diagnostic procedures for non-small-cell lung cancer (NSCLC): Recommendations of the European Expert Group," *Thorax*, vol. 71, no. 2, pp. 177–184, 2016.

[22] J. J. Wang, K. F. Lei, and F. Han, "Tumor microenvironment: Recent advances in various cancer treatments," *Eur. Rev. Med. Pharmacol. Sci.*, vol. 22, no. 12, pp.

3855–3864, 2018.

[23] F. Chen *et al.*, “New horizons in tumor microenvironment biology: Challenges and opportunities,” *BMC Med.*, vol. 13, no. 1, 2015.

[24] E. Jiang, T. Yan, Z. Xu, and Z. Shang, “Tumor Microenvironment and Cell Fusion,” *Biomed Res. Int.*, vol. 2019, pp. 1–12, 2019.

[25] M. R. Junttila and F. J. De Sauvage, “Influence of tumour micro-environment heterogeneity on therapeutic response,” *Nature*, vol. 501, no. 7467, pp. 346–354, 2013.

[26] C. Fernandes, D. Suares, and M. C. Yergeri, “Tumor Microenvironment Targeted Nanotherapy,” *Front. Pharmacol.*, vol. 9, no. October, pp. 1–25, 2018.

[27] N. E. Sounni and A. Noel, “Targeting the tumor microenvironment for cancer therapy,” *Clin. Chem.*, vol. 59, no. 1, pp. 85–93, 2013.

[28] A. E. Denton, E. W. Roberts, and D. T. Fearon, “Stromal Cells in the Tumor Microenvironment,” in *Stromal Immunology*, 1060th ed., L. M. Owens B., Ed. Springer, Cham, 2018, pp. 99–114.

[29] M. Wang *et al.*, “Role of tumor microenvironment in tumorigenesis,” *J. Cancer*, vol. 8, no. 5, pp. 761–773, 2017.

[30] C. Belli *et al.*, “Targeting the microenvironment in solid tumors,” *Cancer Treat. Rev.*, vol. 65, pp. 22–32, 2018.

[31] C. P. De Bock K, Cauwenberghs S, “Vessel abnormalization: another hallmark of cancer?: Molecular mechanisms and therapeutic implications,” *Curr. Opin. Genet. Dev.* , vol. 21, no. 1, pp. 73–79, 2011.

[32] G. Motz, G. T. & Coukos, “The parallel lives of angiogenesis and immunosuppression: cancer and other tales,” *Nat. Rev. Immunol*, vol. 11, pp. 702–711, 2011.

[33] R. S. Ferrara, N. Kerbel, “Angiogenesis as a therapeutic target.,” *Nature*, vol. 438, pp. 967–974, 2005.

[34] D. M. Pardoll, “The blockade of immune checkpoints in cancer immunotherapy,” *Nat. Rev. Cancer* , vol. 12, no. 4, pp. 252–264, 2012.

[35] D. Hu *et al.*, “Heterogeneity of aberrant immunoglobulin expression in cancer cells,” *Cell. Mol. Immunol.*, vol. 8, no. 6, pp. 479–485, 2011.

[36] A. A. Mantovani, A. & Sica, “Macrophages, innate immunity and cancer: balance, tolerance, and diversity.,” *Curr Opin Immunol.*, vol. 22, no. 2, pp. 231–

237, 2010.

[37] D. C. Hinshaw and L. A. Shevde, “The Tumor Microenvironment Innately Modulates Cancer Progression,” *Cancer Res.*, pp. 1–11, 2019.

[38] M. Binnewies *et al.*, “Understanding the tumor immune microenvironment (TIME) for effective therapy.,” *Nat. Med.*, vol. 24, no. 5, pp. 541–550, 2018.

[39] S. Burugu, A. R. Dancsok, and T. O. Nielsen, “Emerging targets in cancer immunotherapy,” *Semin. Cancer Biol.*, vol. 52, no. September 2017, pp. 39–52, 2018.

[40] L. Q. Graves EE, Maity A, “The Tumor Microenvironment in Non-Small Cell Lung Cancer,” *Semin. Radiat. Oncol.*, vol. 20, no. 3, pp. 156–163, 2010.

[41] B.-H. M. Mittal V, El Rayes T, Narula N, McGraw TE, Altorki NK, “The Microenvironment of Lung Cancer and Therapeutic Implications,” *Microenviron. Lung Cancer Ther. Implic.*, vol. 890, pp. 75–110, 2016.

[42] J. Ye *et al.*, “Oxymatrine and cisplatin synergistically enhance anti-tumor immunity of CD8+ T cells in non-small cell lung cancer,” *Front. Oncol.*, vol. 8, no. DEC, pp. 1–11, 2018.

[43] L. Q. Chow, “Exploring Novel Immune-Related Toxicities and Endpoints with Immune-Checkpoint Inhibitors in Non-Small Cell Lung Cancer,” *Am. Soc. Clin. Oncol. Educ. B.*, vol. 33, pp. e280–e286, 2013.

[44] D. B. F. Lieping Chen, “Molecular mechanisms of T cell co-stimulation and co-inhibition,” *Nat. Rev. Immunol.*, vol. 13, no. 4, pp. 227–242, 2013.

[45] N. Villanueva and L. Bazhenova, “New strategies in immunotherapy for lung cancer: beyond PD-1/PD-L1,” *Therapeutic Advances in Respiratory Disease*, vol. 12. 2018.

[46] L. I. X. Ia, Y. U. L. Iu, and Y. I. N. G. W. Anga, “PD-1/PD-L1 Blockade Therapy in Advanced Non-Small-Cell Lung Cancer: Current Status and Future Directions,” *Oncologist*, vol. 24, no. Suppl 1, pp. S31–S41, 2019.

[47] S. Yang, Z. Zhang, and Q. Wang, “Emerging therapies for non-small cell lung cancer,” *J. Hematol. Oncol.*, vol. 12, no. 1, pp. 1–24, 2019.

[48] T. F. B. Ashwin Somasundaram, “The next generation of immunotherapy: keeping lung cancer in check.,” *J. Hematol. Oncol.*, vol. 10, p. 87, 2017.

[49] J. F. G. BENJAMIN HERZBERG, MEGHAN J. CAMPO, “Immune checkpoint inhibitors in non-small cell lung cancer,” *Oncologist*, vol. 22, pp. 81–88, 2017.

[50] J. Borst, J. Hendriks, and Y. Xiao, "CD27 and CD70 in T cell and B cell activation," *Current Opinion in Immunology*, vol. 17, no. 3. pp. 275–281, Jun-2005.

[51] M. Kuka, I. Munitic, M. L. Giardino Torchia, and J. D. Ashwell, "CD70 Is Downregulated by Interaction with CD27," *J. Immunol.*, vol. 191, no. 5, pp. 2282–2289, Sep. 2013.

[52] M. F. Al Sayed *et al.*, "CD70 reverse signaling enhances NK cell function and immunosurveillance in CD27-expressing B-cell malignancies," *Blood*, vol. 130, no. 3, pp. 297–309, Jul. 2017.

[53] K. Zwaenepoel *et al.*, "CD70 and PD-L1 in anaplastic thyroid cancer – promising targets for immunotherapy," *Histopathology*, vol. 71, no. 3, pp. 357–365, Sep. 2017.

[54] T. A. Fehniger, "CD70 turns on NK cells to attack lymphoma," *Blood*, vol. 130, no. 3. American Society of Hematology, pp. 238–239, 20-Jul-2017.

[55] J. Jacobs *et al.*, "Unlocking the potential of CD70 as a novel immunotherapeutic target for non-small cell lung cancer," *Oncotarget*, vol. 6, no. 15, pp. 13462–13475, 2015.

[56] J. Jacobs *et al.*, "Unveiling a CD70-positive subset of cancer-associated fibroblasts marked by pro-migratory activity and thriving regulatory T cell accumulation," *Oncoimmunology*, vol. 7, no. 7, Jul. 2018.

[57] S. P. Ruf M, Mittmann C, Nowicka AM, Hartmann A, Hermanns T, Poyet C, van den Broek M, Sulser T, Moch H, "pVHL/HIF-Regulated CD70 Expression Is Associated with Infiltration of CD27 þ Lymphocytes and Increased Serum Levels of Soluble CD27 in Clear Cell Renal Cell Carcinoma," *Clin Cancer Res.*, vol. 21, no. 4, pp. 889–98, 2015.

[58] L. B. Jilaveanu, J. Sznol, S. A. Aziz, D. Duchen, H. M. Kluger, and R. L. Camp, "CD70 expression patterns in renal cell carcinoma," *Hum. Pathol.*, vol. 43, no. 9, pp. 1394–1399, Sep. 2012.

[59] M. H. J. Van Oers *et al.*, "Expression and release of CD27 in human B-cell malignancies," *Blood*, vol. 82, no. 11, pp. 3430–3436, 1993.

[60] S. Inoue *et al.*, "CD70 expression in tumor-associated fibroblasts predicts worse survival in colorectal cancer patients," *Virchows Arch.*, 2019.

[61] C. Pich *et al.*, "Melanoma-expressed CD70 is involved in invasion and

metastasis," *Br. J. Cancer*, vol. 114, no. 1, pp. 63–70, Jan. 2016.

[62] J. H. W. Pahl *et al.*, "Expression of the immune regulation antigen CD70 in osteosarcoma," *Cancer Cell Int.*, vol. 15, no. 1, Mar. 2015.

[63] C. Claus, C. Riether, C. Schürch, M. S. Matter, T. Hilmenyuk, and A. F. Ochsenbein, "CD27 signaling increases the frequency of regulatory T cells and promotes tumor growth," *Cancer Res.*, vol. 72, no. 14, pp. 3664–3676, Jul. 2012.

[64] C. L. Law *et al.*, "Lymphocyte activation antigen CD70 expressed by renal cell carcinoma is a potential therapeutic target for anti-CD70 antibody-drug conjugates," *Cancer Res.*, vol. 66, no. 4, pp. 2328–2337, Feb. 2006.

ETHICS COMMITTEE APPROVAL

T.C.
İSTANBUL ÜNİVERSİTESİ
İSTANBUL TIP FAKÜLTESİ
KLİNİK ARAŞTIRMALAR ETİK KURULU

Sayı : 913 Tarih : 23.08.2017
Konu: Prof. Dr. İlhan YAYLIM hk.

Sayın Prof. Dr. İlhan YAYLIM
Aziz Sancar Deneysel Tıp Araştırma Enstitüsü

İlgi : Moleküler Tıp Anabilim Dalının 07/08/2017 gün ve 296972 sayılı yazısı

Sorumlu araştırıcılığını üstlendiğiniz ve Merve Saide UZUNOĞLU' nun yürüteceği 2017/884 dosya numaralı "Küçük hücreli dışı akciğer kanserli hastalarda CD70/CD27 molekülleri ile ilişkili mekanizmaların incelenmesi" başlıklı çalışma kurulumuzun 11/08/2017 gün ve 13 sayılı toplantısında görüşülerek etik yönden uygun bulunmuş olup, tutanaklar ekte sunulmuştur.

Bilgilerinizi rica ederim.

Prof. Dr. A.Yağız ÜRESİN
İstanbul Tıp Fakültesi Klinik Araştırmalar
Etik Kurul Başkanı

Ekl: İstanbul Tıp Fakültesi Klinik Araştırmaları Etik Kurulu Karar Formu

İSTANBUL TIP FAKÜLTESİ KLİNİK ARAŞTIRMALARI ETİK KURULU KARAR FORMU

ETİK KURUL BİLGİLERİ	ETİK KURULUN ADI	**İSTANBUL TIP FAKÜLTESİ KLİNİK ARAŞTIRMALARI ETİK KURULU**
	AÇIK ADRESİ:	**İ.Ü.İSTANBUL TIP FAKÜLTESİ HULUSİ BEHÇET KÜTÜPHANESİ KAT:3 FATİH/İSTANBUL**
	TELEFON	**0 (212) 414 21 53**
	FAKS	**0 (212) 414 21 53**
	E-POSTA	**itfetikkurul@istanbul.edu.tr.**

BAŞVURU BİLGİLERİ	ARAŞTIRMANIN AÇIK ADI	**"Küçük hücreli dışı akciğer kanserli hastalarda CD70/CD27 molekülleri ile ilişkili mekanizmaların incelenmesi"**			
	ARAŞTIRMA PROTOKOL KODU	---			
	KOORDİNATÖR/SORUMLU ARAŞTIRMACI UNVANI/ADI/SOYADI	**Prof. Dr. İlhan YAYLIM**			
	KOORDİNATÖR/SORUMLU ARAŞTIRMACININ UZMANLIK ALANI	**Moleküler Tıp**			
	KOORDİNATÖR/SORUMLU ARAŞTIRMACININ BULUNDUĞU MERKEZ	**İstanbul Üniversitesi Aziz Sancar Deneysel Tıp Araştırma Enstitüsü Moleküler Tıp Anabilim Dalı**			
	DESTEKLEYİCİ	**İstanbul Üniversitesi Bilimsel Araştırma Projeleri**			
	DESTEKLEYİCİNİN YASAL TEMSİLCİSİ	---			
	ARAŞTIRMANIN FAZI	FAZ 1	☐		
		FAZ 2	☐		
		FAZ 3	☐		
		FAZ 4	☐		
	ARAŞTIRMANIN TÜRÜ	Yeni Bir Endikasyon	☐		
		Yüksek Doz Araştırması	☐		
		Diğer ise belirtiniz :			
	ARAŞTIRMAYA KATILAN MERKEZLER	TEK MERKEZ ☐	ÇOK MERKEZLİ ■	ULUSAL ■	ULUSLARARASI ☐

İSTANBUL TIP FAKÜLTESİ KLİNİK ARAŞTIRMALARI ETİK KURULU KARAR FORMU

ARAŞTIRMANIN AÇIK ADI	"Küçük hücreli dışı akciğer kanserli hastalarda CD70/CD27 molekülleri ile ilişkili mekanizmaların incelenmesi"

	Belge Adı	Tarihi	Versiyon Numarası	Dili
DEĞERLENDİRİLEN BELGELER	ARAŞTIRMA PROTOKOLÜ	01/08/2017		Türkçe ■ İngilizce ☐ Diğer☐
	BİLGİLENDİRİLMİŞ GÖNÜLLÜ OLUR FORMU	■		Türkçe ■ İngilizce ☐ Diğer☐
	OLGU RAPOR FORMU	☐		Türkçe ☐ İngilizce ☐ Diğer☐
	ARAŞTIRMA BROŞÜRÜ	☐		Türkçe ☐ İngilizce ☐ Diğer☐
DEĞERLENDİRİLEN DİĞER BELGELER	**Belge Adı**	☐	**Açıklama**	
	TÜRKÇE ETİKET ÖRNEĞİ	☐		
	SİGORTA	☐		
	ARAŞTIRMA BÜTÇESİ	■		
	BİYOLOJİK MATERYEL TRANSFER FORMU	☐		
	HASTA KARTI/GÜNLÜKLERİ	☐		
	İLAN	☐		
	YILLIK BİLDİRİM	☐		
	SONUÇ RAPORU	☐		
	GÜVENLİLİK BİLDİRİMLERİ	☐		
	DİĞER:	■	Anabilim Dalı Başkanlığından Üst Yazı ve Akademik Kurul Kararı, Literatür Kaynağı, Sorumluluk Paylaşım Belgesi, Olgu Rapor Formu, İlgili Elemanların Bilgilendirildiğine Dair Belge, CV, CD	
KARAR BİLGİLERİ	**Karar No:13**	**Tarih: 11/08/2017**		
	İstanbul Üniversitesi Aziz Sancar Deneysel Tıp Araştırma Enstitüsü Moleküler Tıp Anabilim Dalında görevli **Prof. Dr. İlhan YAYLIM' ın** sorumluluğunda ve Merve Saide UZUNOĞLU' nun yürüteceği yukarıda bilgileri verilen araştırma başvuru dosyası ile ilgili belgeler araştırmanın gerekçe, amaç, yaklaşım ve yöntemleri dikkate alınarak incelenmiş, gerçekleştirilmesinde etik ve bilimsel sakınca bulunmadığına toplantıya katılan Etik Kurul üye tam sayısının salt çoğunluğu ile karar verilmiştir.		

İSTANBUL TIP FAKÜLTESİ KLİNİK ARAŞTIRMALARI ETİK KURULU	
ÇALIŞMA ESASI	**19.08.2011 tarihli, 28030 sayılı Resmi Gazetede yayınlanan Klinik Araştırmalar Hakkındaki Yönetmelik**
BAŞKANIN UNVANI / ADI / SOYADI:	**Prof. Dr. A. Yağız ÜRESİN**

Unvanı/Adı/Soyadı	Uzmanlık Alanı	Kurumu	Cinsiyet		Araştırma ile ilişki *		Katılım **		İmza
Prof. Dr. A. Yağız ÜRESİN	Farmakoloji ve Klinik Farmakoloji	İstanbul Tıp Fakültesi (Etik Kurul Başkanı	E ■	K ☐	E ☐	H ■	E ■	H ☐	
Prof. Dr. Berrin UMMAN	Kardiyoloji	İstanbul Tıp Fakültesi (Etik Kurul Başkan Yardımcısı)	E ☐	K ■	E ☐	H ■	E ☐	H ■	İZİNLİ
Prof. Dr. Ahmet GÜL	Romatoloji	İstanbul Tıp Fakültesi	E ■	K ☐	E ☐	H ■	E ■	H ☐	
Prof. Dr. Oğuzhan ÇOBAN	Nöroloji	İstanbul Tıp Fakültesi	E ■	K ☐	E ☐	H ■	E ■	H ☐	
Dr. Sevda ÖZEL YILDIZ	Biyoistatistik	İ.Ü. İstanbul Tıp Fakültesi Biyoistatistik	E ☐	K ■	E ☐	H ■	E ☐	H ■	İZİNLİ

* :Araştırma ile İlişki
** :Toplantıda Bulunma

İ.Ü. İstanbul Tıp Fakültesi Klinik araştırmalar Etik kurulu 13.04.2013 tarih, 28617 sayılı Resmi Gazetede yayınlanan Klinik Araştırmalar Hakkında Yönetmelik çerçevesinde kurulmuş ve T.C. Sağlık Bakanlığı Türkiye İlaç ve Tıbbi Cihaz Kurumu tarafından onaylanmıştır. İlgili yönetmelik kapsamında kalan araştırmalar Sağlık Bakanlığından izin almak zorundadır. Yönetmelik kapsamı dışında kalan araştırmalar ise Etik Kurul bünyesinde oluşturulmuş 5 kişilik alt komisyon tarafından değerlendirilmekte olup Sağlık Bakanlığı izninе tabi değildir.

FIRST PAGE OF PLAGIARISM REPORT

INVESTIGATION OF CD70-CD27 RELATED MOLECULAR MECHANISMS IN TUMOR MICROENVIRONMENT OF NON-SMALL CELL LUNG CANCER

ORIJINALLIK RAPORU

%4	%2	%2	%2
BENZERLIK ENDEKSI	İNTERNET KAYNAKLARI	YAYINLAR	ÖĞRENCI ÖDEVLERI

BIRINCIL KAYNAKLAR

1	Submitted to University of Sheffield Öğrenci Ödevi	<%1
2	www.oncotarget.com İnternet Kaynağı	<%1
3	tessera.spandidos-publications.com İnternet Kaynağı	<%1
4	Submitted to Sheffield Hallam University Öğrenci Ödevi	<%1
5	Submitted to University of Birmingham Öğrenci Ödevi	<%1
6	Julie Jacobs, Karen Zwaenepoel, Christian Rolfo, Jolien Van den Bossche et al. "Unlocking the potential of CD70 as a novel immunotherapeutic target for non-small cell lung cancer", Oncotarget, 2015 Yayın	<%1

CURRICULUM VITAE

Kişisel Bilgiler

Adı	Merve	**Soyadı**	Uzunoğlu
Doğ.Yeri	İzmir	**Doğ.Tar.**	05.04.1993
Email	mervesuzunoglu@gmail.com	**Uyruğu**	Türk

Eğitim Düzeyi

	Mezun Olduğu Kurumun Adı	**Mez. Yılı**
Doktora		
Yük.Lis.		
Lisans		
Lise		

İş Deneyimi (Sondan geçmişe doğru sıralayın)

	Görevi	**Kurum**	**Süre (Yıl - Yıl)**
1.			-
2.			-
3.			-

Yabancı Dilleri	**Okuduğunu Anlama***	**Konuşma***	**Yazma***	**KPDS/ÜDS Puanı**	**(Diğer) Puanı**

***Çok iyi, iyi, orta, zayıf olarak değerlendirin

	Sayısal	**Eşit Ağırlık**	**Sözel**
ALES Puanı			
(Diğer) Puanı			

Bilgisayar Bilgisi

Program	**Kullanma becerisi**
Microsoft Office	Çok iyi
GraphPad Prism	İyi
ImageJ	Çok iyi

Yayınları/Tebligleri Sertifikaları/Ödülleri

Özel İlgi Alanları (Hobileri):